

Morphological evolution of the hominid brain

Michelangelo Bisconti^{1,2,*}, Giandonato Tartarelli³

Academic Editor: Gabriel Gutiérrez-Ospina

Abstract

A comparative analysis of the brain surfaces and endocasts of 35 hominid specimens including 24 operational taxonomic units was performed with the aim to search for morphological transformations of the brain surface that occurred over time throughout the hominid lineage. Our research was directed at size-independent morphological characters. We found 14 characters dealing with (1) relative proportions of the frontal lobe, (2) relative proportions of the parietal lobe, (3) relative proportions of the temporal lobe, (4) extension of the occipital lobe and position of the parieto-occipital sulcus, and (5) morphology and proportions of the frontal lobe. We described and mapped these characters onto a reference phylogeny of Hominidae including 4 ape species and 20 operational taxonomic units belonging to bipedal hominins (species *Australopithecus*, *Paranthropus*, and *Homo*) to infer character states at the ancestral nodes. At the macroscopical level, we found that (a) the occipital lobe changed its inclination at the *Pan-Australopithecus* transition; (b) the frontal lobe increased its roundness during the transition between *Australopithecus/Paranthropus* and *Homo*; (c) the parietal lobe increased its relative length in a hominin clade including *Homo erectus*, *H. floresiensis*, *H. cepranensis*, *H. neandertalensis* and *H. sapiens*; and (d) the distal border of the temporal lobe increased its height and the posterolateral border of the temporal lobe acquired a ventrally concave outline in the clade including *H. neandertalensis* and *H. sapiens*. These observations are important in the broader context of the inference of the relationships of paleoneurology and behavioral outputs in extinct hominid species.

Keywords: *Australopithecus*, brain, endocast, fossil, *Homo*, paleoanthropology, *Paranthropus*

Citation: Bisconti M, Tartarelli G. Morphological evolution of the hominid brain. *Academia Biology* 2025;3. <https://doi.org/10.20935/AcadBiol7710>

1. Introduction

According to morphological and genetic studies, the Hominidae clade includes both apes and humans and encompasses a range of different morphological and physiological characters enabling hominid species to live in a wildly diversified set of habitats [1]. Apes, humans, and their extinct relatives known by their fossil record are characterized by a range of morphological differences that comprise both skeletal and soft tissues including the brain. In particular, the latter represents the most prominent diagnostic character for defining our species, *Homo sapiens*, in the common thought of non-scholars in the field because of its relative size. The human brain, indeed, is particularly large with respect to the whole-body mass and this fact may be quantified by the Encephalization Quotient (EQ) originally developed by Jerison [2]. The EQ variation across mammal groups has been analyzed in the last fifty years, showing that in modern humans, the EQ ~ 6.7 and is higher than those of all the other mammalian species [3]. Surprisingly, even though apes are the most closely related mammalian species to *Homo*, they are not particularly encephalized. Apart from humankind, the most encephalized mammals include five species of dolphins [4] whose EQ ranges from 5 to 5.7 and whose encephalization reached human-like EQ values already during the Miocene, about 15 million years ago [4, 5].

In the last half century, many papers were published dealing with EQ evolution in mammals, primates, and other vertebrates, but

relatively few were about the evolution of brain morphology. Up to about ten years ago, most papers dealing with the characteristics of the brain of fossil species had to rely on natural or human-made skull endocasts, but presently, the availability of non-invasive techniques allows the digital reconstruction of three-dimensional models of endocasts of intact skulls, and this availability is generating a wealth of new data about the morphological evolution of the brain in all vertebrates (e.g., [6, 7]). Techniques like CT scans and magnetic resonance analysis provide a lot of new information about endocranial anatomy, the morphology of the complex formed by the brain and meninges including part of the endocranial vasculature (e.g., [8, 9]), and the sensory anatomy with special emphasis on the inner ear (e.g., [10, 11]). However, a new synthesis of morphological data from natural and digital endocasts has not been attempted on primate brain evolution up to now. Such a synthesis would be of great benefit because it would allow the eventual changes in the surface morphology of the main brain characters to be visualized, which, in turn, could contribute to explaining aspects related to the evolution of human cognition.

To better explain this point, it is necessary to remark that the surface morphology of the brain is characterized by an intricate folding of the external cellular layer where the bodies of the cortical neurons are located; this layer is known as the cortex or gray matter. The folding is not chaotic but genetically organized,

¹Department of Engineering and Geology, "G. D'Annunzio" University of Chieti-Pescara, 66100 Chieti, Italy.

²San Diego Natural History Museum, San Diego, CA 92101, USA.

³Scuola Normale Superiore, 56126 Pisa, Italy.

*email: michelangelo.bisconti@unich.it

showing a repetitive sulcal pattern that is shared in part with non-primate mammals [12]. Different areas of the brain surface can be structurally and functionally separated based on spatial differences in their cytoarchitectures [13]; these areas are responsible for different cognitive, sensory, and motor functional outputs. The mosaic of these areas may show some differences in the brains of different species as some areas may be absent from certain taxa and overdeveloped in others. Some of these areas can be observed in natural and digital endocasts and the origins of their morphologies and topological relationships can be traced back in time thanks to the paleontological record as far as the brain surface is concerned (e.g., [12, 14]). These observations represent the theoretical ground of our work aimed at determining the evolution of the cerebral surface through the geological time of hominid evolution.

Towards this goal, here, we perform an analysis of the distribution of characters of both the brains and the skull endocasts of four ape species (*Pongo pygmaeus*, *Gorilla gorilla*, *Gorilla beringei*, and *Pan troglodytes*) and several australopithecine and human species in the context of a morphology-based phylogenetic hypothesis of hominid evolution [see below, Section 2]. Our objective is to individuate the eventual occurrence of morphological transformations of the brain surface in Hominidae over the last 7–10 million years, a time that represents the inferred divergence date of the hominins (including australopithecines and humans) from their sister group. Our search is about characters that are thought to be unrelated to the evolution of absolute brain size and is aimed at providing new information about the last stages of the assembly of the brain of our species.

2. Materials and methods

2.1. Phylogenetic hypothesis

To base our comparative analysis, we adopted a simplified phylogenetic hypothesis of hominid relationships based on recent research (**Figure 1A**). In that simplified phylogeny, we included three ape species with four species (*Pongo pygmaeus*, *Gorilla gorilla*, *Gorilla beringei*, and *Pan troglodytes*). The relationships of these taxa were those inferred by ref. [15]; the divergence dates of the ape taxa are from ref. [16]. The hominins not belonging to *Homo* included most of the species belonging to *Australopithecus* and *Paranthropus*. The relationships of these taxa were obtained from ref. [15] including the sister group relationships of *Australopithecus sediba* and *Homo*. The divergence date of bipedal hominins from apes was from ref. [17]. The relationships of the species belonging to *Homo* presented in **Figure 1A** were a synthesis of the more detailed analyses published by refs. [18–22]. We report a specimen-based version of the simplified phylogeny in **Figure 1B** showing the specimens used in the comparative analysis (**Figure 1B**). We understand that there is not a full consensus about the relationships of at least some of the human species described up until now and, for this reason, we adopted a phylogenetic hypothesis that is a compromise of some of the results coming from the recent literature. Data on the specimens used here and their stratigraphic and geographic ranges are provided in **Table 1** together with the literature used for the comparative analysis of brains and endocasts.

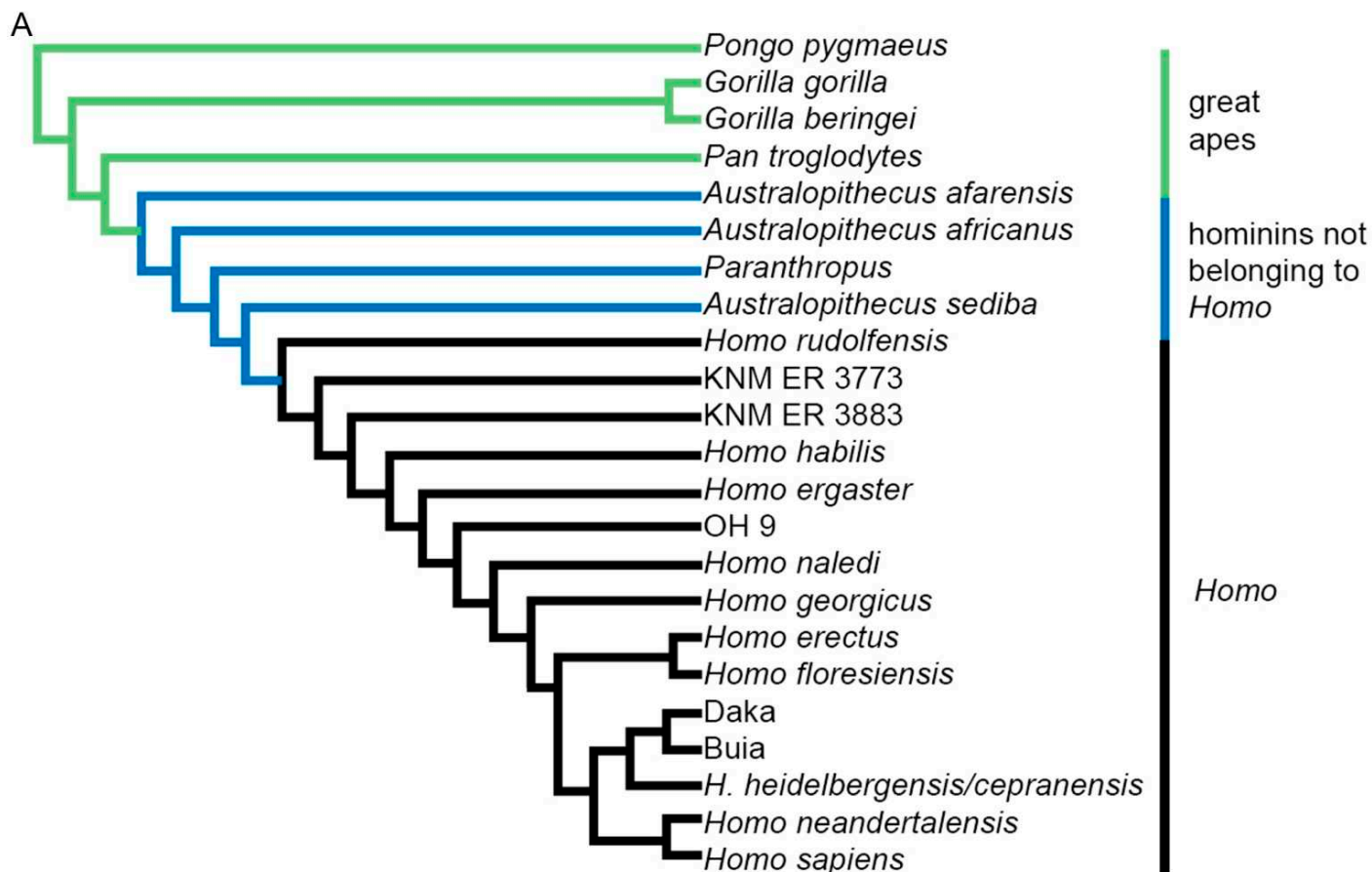


Figure 1 • Cont.

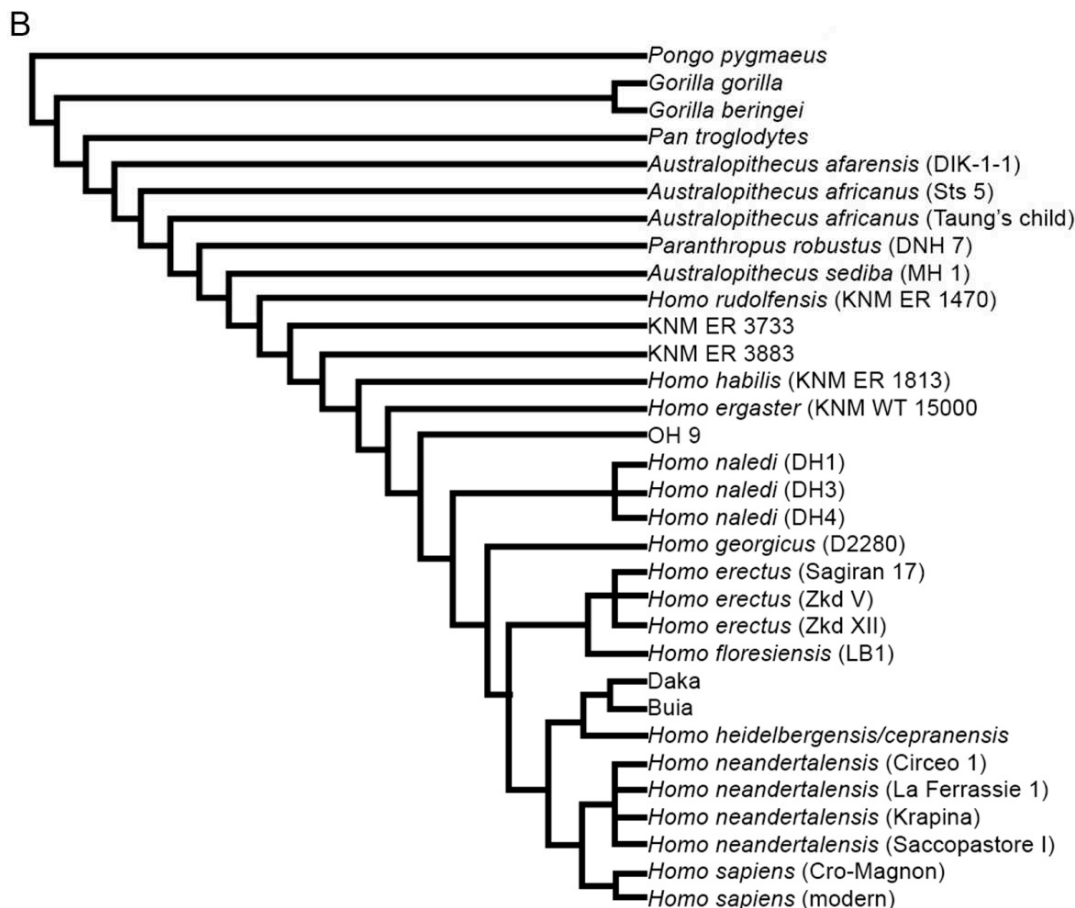


Figure 1 • The reference phylogeny used in the present paper. (A) Species phylogeny. (B) Specimen-based phylogeny.

Table 1 • Morphological sample used in present paper.

N.	Taxonomy	Specimen	Stratigraphic age	Geographic range	Brain volume (cc)	References on brains and endocasts
1	<i>Pongo pygmaeus</i>		Recent	East Asia	323 ¹	[23, 24]
2	<i>Gorilla gorilla</i>	Many specimens	Recent	West Central Africa	504	[25]
3	<i>Gorilla beringei</i>	Many specimens	Recent	Central Africa	450	[25]
4	<i>Pan troglodytes</i>		Recent	Central and Eastern Africa	320–370 ¹	[26]
5	<i>Pan troglodytes</i>	YN-77-111	Recent	Central and Eastern Africa	388.96	[25]
6	<i>Pan troglodytes</i>	YN-92-115	Recent	Central and Eastern Africa	364.8	[27]
7	<i>Pan troglodytes</i>		Recent	Central and Eastern Africa	320–370 ¹	[28]
8	<i>Australopithecus afarensis</i>	DIK-1-1	Mid-Pliocene (c. 3.3 Ma)	East Central Africa	275	[26]
9	<i>Australopithecus africanus</i>	Taung child	Latest Pliocene (c. 2.8 Ma)	South Africa	382	[29, 30]
10	<i>Australopithecus africanus</i>	Sts 5	Latest Pliocene (c. 2.5 Ma)	South Africa	475	[31, 32]
11	<i>Australopithecus sediba</i>	MH1	Middle Pleistocene (c. 1.8 Ma)	South Africa	420	[33]
12	<i>Paranthropus robustus</i>	DNH 7	Early-Middle Pleistocene (c. 2.3–1.2 Ma)	South Africa	450	[34]
13	<i>Homo rudolfensis</i>	KNM ER 1470	Early Pleistocene (c. 2 Ma)	North-Eastern Africa	752	[35, 36]
14	KNM ER 3733	KNM ER 3733	Early-Middle Pleistocene (c. 1.7 Ma)	North-Eastern Africa	848	[9, 36]

Table 1 • Cont.

N.	Taxonomy	Specimen	Stratigraphic age	Geographic range	Brain volume (cc)	References on brains and endocasts
15	KNM ER 3883	KNM ER 3883	Early-Middle Pleistocene (c. 1.5 Ma)	North-Eastern Africa	804	[9, 36]
16	<i>Homo habilis</i>	KNM ER 1813	Early Pleistocene (c. 1.9 Ma)	North-Eastern Africa	510	[9, 36]
17	OH9	OH9	Early-Middle Pleistocene (c. 1.4 Ma)	East Central Africa	1067	[36, 37]
18	<i>Homo ergaster</i>	KNM WT 15000	Early-Middle Pleistocene (c. 1.5 Ma)	North-Eastern Africa	880	[9, 37]
19	<i>Homo georgicus</i>	D2280	Earliest Pleistocene (c. 1.8 Ma)	Central Asia	790	[9]
20	<i>Homo naledi</i>	DH1	Late-Middle Pleistocene (c. 0.33–0.36 Ma)	South Africa	555	[38]
21	<i>Homo naledi</i>	DH3	Late-Middle Pleistocene (c. 0.33–0.36 Ma)	South Africa	460	[38]
22	<i>Homo naledi</i>	DH4	Late-Middle Pleistocene (c. 0.33–0.36 Ma)	South Africa	?	[38]
23	<i>Homo erectus</i>	Sangiran 17	Middle Pleistocene (c. 0.7 Ma)	East Asia	1004	[9, 37]
24	<i>Homo erectus</i>	Zkd V	Late Pleistocene (c. 0.29 Ma)	East Asia	1140	[37]
25	<i>Homo erectus</i>	Zkd XII	Late Pleistocene (c. 0.075 Ma)	East Asia	1030	[37, 39]
26	<i>Homo floresiensis</i>	LB1	Late Pleistocene (c. 0.19–0.054 ka)	East Asia	417	[38, 40]
27	Daka	BOU-VP-2/66	Middle Pleistocene (c. 1 Ma)	East Central Africa	1000 ²	[41]
28	Buia		Middle Pleistocene (c. 1 Ma)	East Central Africa	800	[8, 9]
29	<i>Homo cepranensis</i>		Late Middle Pleistocene (c. 0.5 Ma)	Central-Southern Europe (Italy)	1185 ²	[22, 42]
30	<i>Homo neandertalensis</i>	Saccopastore I	Late Pleistocene (c. 0.13–0.1 Ma)	Central-Southern Europe (Italy)	1174	[43]
31	<i>Homo neandertalensis</i>	Krapina 3	Late Pleistocene (c. 0.13 Ma)	Central Europe (Croatia)	1255	[43]
32	<i>Homo neandertalensis</i>	Circeo I	Latest Pleistocene (c. 0.05 Ma)	Central-Southern Europe (Italy)	1350	[35, 44]
33	<i>Homo neandertalensis</i>	La Ferrassie I	Latest Pleistocene (c. 0.05 Ma)	Central-Western Europe (France)	1268	[35, 45]
34	<i>Homo sapiens</i>	Cro-Magnon 1	Latest Pleistocene (0.03 Ma)	West Europe (France)	1514 ³	[14]
35	<i>Homo sapiens</i>		Recent	Worldwide	1478	[14, 28]

¹ Mean values from [28]; ² original data in mL converted in cc by us; ³ mean value from $N = 13$ individuals from [14]. The symbol “?” indicates that the value was not provided in the literature and is unknown.

2.2. Endocasts and brains

The comparative morphological diversity of brains and of their corresponding endocasts was richly illustrated in the past (e.g., [46]). The vertebrate brain includes several portions that are characterized by different morphological characters that can be scored for comparative purposes; the human brain is not different from those of other mammals, in this sense. The human brain includes the telencephalic hemispheres, the cerebellum, the hindbrain, several internal structures and nuclei, and the cranial nerve roots. Even limiting our attention to the telencephalic hemispheres, we observe that different parts are individuated by human anatomy including lobes, fissures, and sulci (e.g., [28, 35]). Most of these structures cannot be observed in the endocasts, because the meninges cover the brain surface. For this reason, here, we focus on a small number

of characters that can be observed in both the brain and its corresponding endocast (**Figure 2**).

In particular, we focus on the following structures: (a) position and shape of the central sulcus (i.e., the fissure of Rolando), (b) morphology of the frontal bec, (c) morphology and position of the temporal lobe, (d) morphology and relative extension of the parietal lobe, (e) position of the parieto-occipital sulcus, (f) position and morphology of the occipital lobe, (g) position of the imprint of the coronal suture in the endocast, and (h) morphology of the orbital surface of the frontal lobe. These characters can be observed in both brains and most endocasts and, together with the overall outline of the telencephalic hemispheres in dorsal, lateral, posterior, and anterior views, contribute to provide a morphological characterization of the brain's general shape as covered by the meninges.

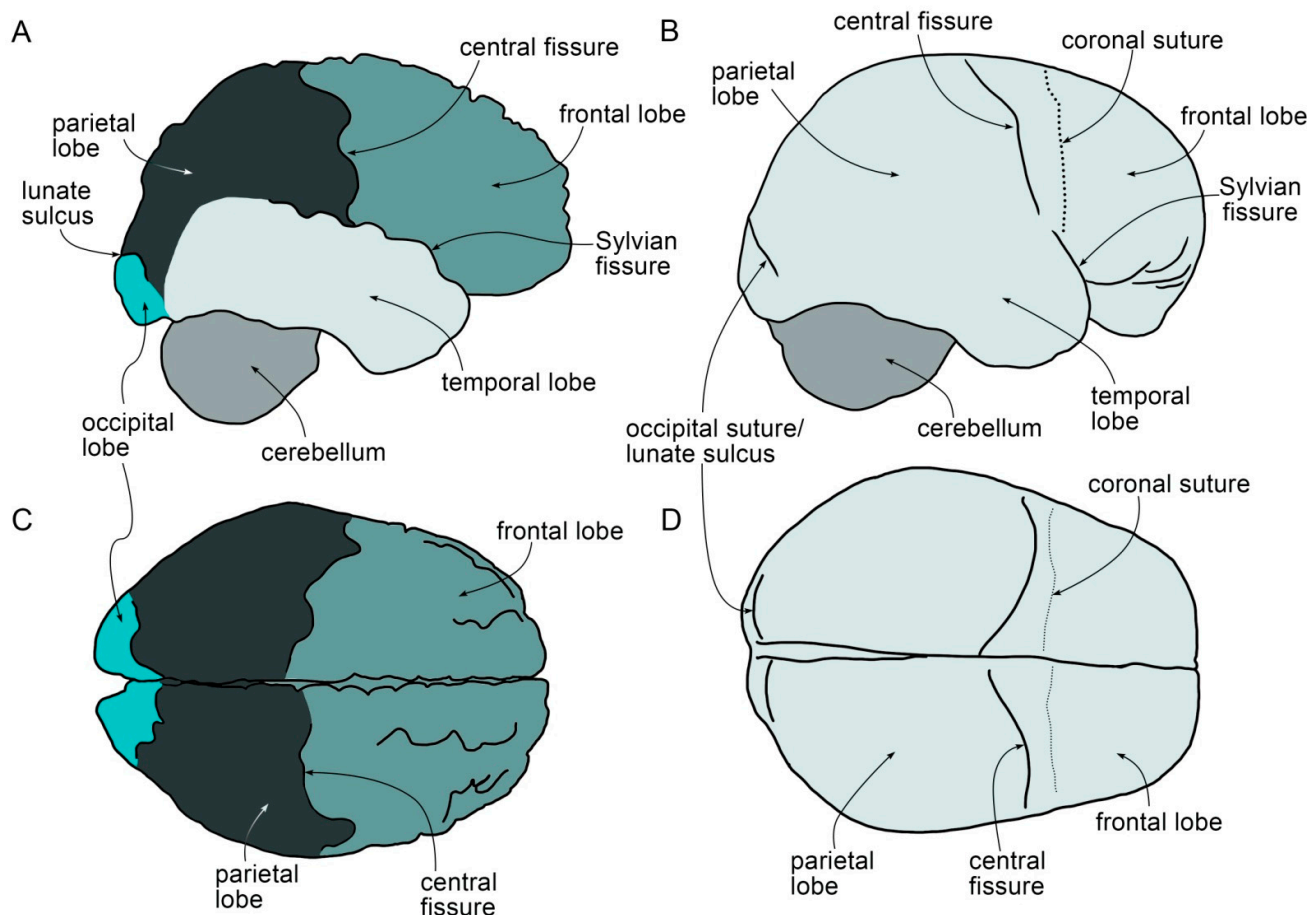


Figure 2 • Gross morphologies of the human brain and differences with the corresponding endocast. (A) The schematic brain in right lateral view. (B) The scheme of the corresponding endocast. (C) The schematic brain in dorsal view. (D) The scheme of the corresponding endocast.

We obtained schemes from the original images of brains and endocasts in lateral, dorsal, anterior, and posterior views from the numerous sources listed in **Table 1**. The schemes for modern *Homo sapiens* and *Gorilla* were derived from the endocast morphologies that were published in the references provided in **Table 1**. In particular, the scheme for *Gorilla* was derived from the following procedure: we made a line drawing of the external outline of the two brains mentioned in the ref. of **Table 1** and then we traced the lines corresponding to the Sylvian fissure, the central sulcus, and the parieto-occipital sulcus in the corresponding positions based on the photographic plates provided by the above paper. We realized the scheme for the chimp by following the same method. We realized the schemes with a Wacom Intuos graphic tablet in Adobe Photoshop 2024.

The morphologies of brains and endocasts included in the present work were compared independently from their absolute size but we added the inferred or measured brain sizes in **Table 1** for comparative purposes. We made our observations size-free by comparing schemes of the specimens depicted with the same length between the anterior and the posterior ends of the telencephalic hemispheres; this allowed us to discern eventual relative morphological and size changes in different brain districts.

2.3. Character mapping

The character states individuated through the comparative analysis were described and subsequently coded in the taxon x character

matrix of **Table 2**, which was analyzed by MESQUITE 3.61 [47] against the simplified phylogenetic hypotheses of **Figure 1A,B**. By means of this analysis, we analyzed the distribution of the character states against the adopted phylogenetic hypothesis to trace the character history and to infer morphological transformations at ancestral nodes. Towards this goal, we used the maximum likelihood (ML) algorithm under the Mk1 model of character distribution as implemented in the software.

3. Results

3.1. Brain and endocast diversity in hominids

The sample used in the present paper is illustrated in **Figure 3**, **Figure 4** and **Figure 5**. In lateral view, the outline of the dorsal border of the telencephalic hemispheres appears homogeneously convex in apes, *Homo rudolfensis*, *H. georgicus*, and *H. naledi*; in all the other species, the posterior portion of the hemispheres shows a higher inclination with respect to the horizontal axis. In lateral view, the posterior portion of the hemispheres (corresponding to the occipital lobe) shows a higher dorsoventral development and the posterolateral border of the hemispheres is ventrally concave in KNM ER 3733, KNM ER 3883, OH9, *Homo erectus*, *H. neanderthalensis*, and *H. sapiens* (**Figure 3**). In *Australopithecus*, *Paranthropus*, *Homo habilis*, *H. rudolfensis*, *H. georgicus*, *H. naledi*, and Daka, this ventral development of the occipital lobe is not observed and the posterolateral border of the hemispheres posterior

to the temporal lobe is straight. In lateral view, the central sulcus is dorsoventrally straight to anteriorly convex in apes, *Australopithecus*, *Paranthropus*, *Homo habilis*, *H. rudolfensis*, *H. naledi*, and Buia; in other human species, it may be anteriorly concave or convex. However, in *Homo neandertalensis*, *H. sapiens*, *H. heidelbergensis/cepranensis*, and the previously mentioned species, the dorsal-most portion of the central sulcus is located more posteriorly than the ventral-most portion. This pattern demonstrates an anteroposterior expansion of the dorsal portion of the frontal lobe in *H. neandertalensis*, *H. erectus*, *H. heidelbergensis/cepranensis*, and *H. sapiens* with respect to the other human and non-human hominids. In lateral view, it can be observed that the orbital portion of the frontal lobe (black arrowheads in **Figure 3**) is higher in humans than in non-human specimens, being more developed in *H. sapiens*, *H. neandertalensis*, *H. heidelbergensis/cepranensis*, *H. erectus* (Zkd XII), and OH9.

In dorsal view, we observe that the external outline of the telencephalic hemispheres is uniformly convex in apes, *Australopithecus*,

Paranthropus, *Homo rudolfensis*, *H. naledi*, Buia, and *H. georgicus* (**Figure 4**). In *Homo ergaster*, *H. erectus*, *H. heidelbergensis/cepranensis*, KNM ER 3733, KNM ER 3883, OH9, *H. neandertalensis*, and *H. sapiens*, the lateral outlines of the cerebral hemispheres are sigmoid because of a lateral protrusion of the anterior portion of the temporal lobe that is anteriorly bounded by a lateral concavity that can be observed in dorsal view (white arrowheads in **Figure 4**). In dorsal view, it is possible to observe that the parieto-occipital sulcus is located more anteriorly in apes and more posteriorly in hominins; this means that the distance between the parieto-occipital sulcus and the central sulcus is comparatively shorter in apes than hominins as far as the dorsal portion of the parietal lobe is concerned (this is exemplified by comparison with the brain of *Pan troglodytes* in **Figure 6**). As the ventral-most portion of the central sulcus is located anteriorly in hominins, the anteroposterior length of the parietal lobe is comparatively longer in *Paranthropus* and *Homo*, reaching its maximum in *H. neandertalensis*, *H. sapiens*, *H. heidelbergensis/cepranensis*, and some *H. erectus* specimens (i.e., Zkd XII).

Table 2 • The taxon x character matrix used in the present paper to infer brain and endocast characters at the ancestral nodes.

N.	Species	Specimen(s)	Character states
1	<i>Pongo pygmaeus</i>	See Table 1	00000000000000
2	<i>Gorilla gorilla</i>	See Table 1	00000000000000
3	<i>Gorilla beringei</i>	See Table 1	00000000000000
4	<i>Pan troglodytes</i>	YN-77-111+ YN-92-115 + specimen in Table 1	11000000000000
5	<i>Australopithecus afarensis</i>	DIK-1-1	1101000000002?
6	<i>Australopithecus africanus</i>	Taung child	11000001000000
7	<i>Australopithecus africanus</i>	Sts 5	11100001000020
8	<i>Australopithecus sediba</i>	MH1	???1001100010?
9	<i>Paranthropus robustus</i>	DNH 7	1112??01100001
10	<i>Homo rudolfensis</i>	KNM ER 1470	11000010000110
11	KNM ER 3733	KNM ER 3733	1100??0?011110
12	KNM ER 3883	KNM ER 3883	1111??0?011020
13	<i>Homo habilis</i>	KNM ER 1813	110211000?01?1
14	OH 9	OH 9	1101??010111?0
15	<i>Homo ergaster</i>	KNM WT 15000	110?011???01?0
16	<i>Homo georgicus</i>	D2280	11110001100100
17	<i>Homo erectus</i>	Sangiran 17	111?1101??11?0
18	<i>Homo erectus</i>	Zkd XII	1112??0?111120
19	<i>Homo floresiensis</i>	LB 1	111?000?1?11?0
20	<i>Homo naledi</i>	DH1+DH2+DH3	1000??00000000
21	Buia	Buia	11120101111120
22	Daka	BOU-VP-2/66	?1?101?11???2?
23	<i>Homo cepranensis</i>	See Table 1	11021111 ² 110121
24	<i>Homo neandertalensis</i>	Circeo I+ Saccopastore I+La Ferrassie I+Krapina 3	12 ¹ 12??11110120
25	<i>Homo sapiens</i>	Cro-Magnon 1	12121111110121
26	<i>Homo sapiens</i>	modern	12121111110121

¹ Among the specimens of *Homo neandertalensis* studied in the present paper, Krapina 1 does not show evidence of a strong ventral protrusion of the posterior border of the telencephalic hemispheres; as we found a strong protrusion in all the other examined specimens, we coded the protrusion as strong (state 2) for this species. ² In *Homo cepranensis*, the dorsal end of the central sulcus is not well-defined; we coded it in state 1 based on the overall shape of the preserved portion of the central sulcus and on comparisons with other hominins. We applied the same method to score *Homo erectus* Zkd XII in which the ventral end of the central sulcus is not well-defined. The sign “?” indicates characters that are not preserved in the specimen and that cannot be inferred from comparative analysis.

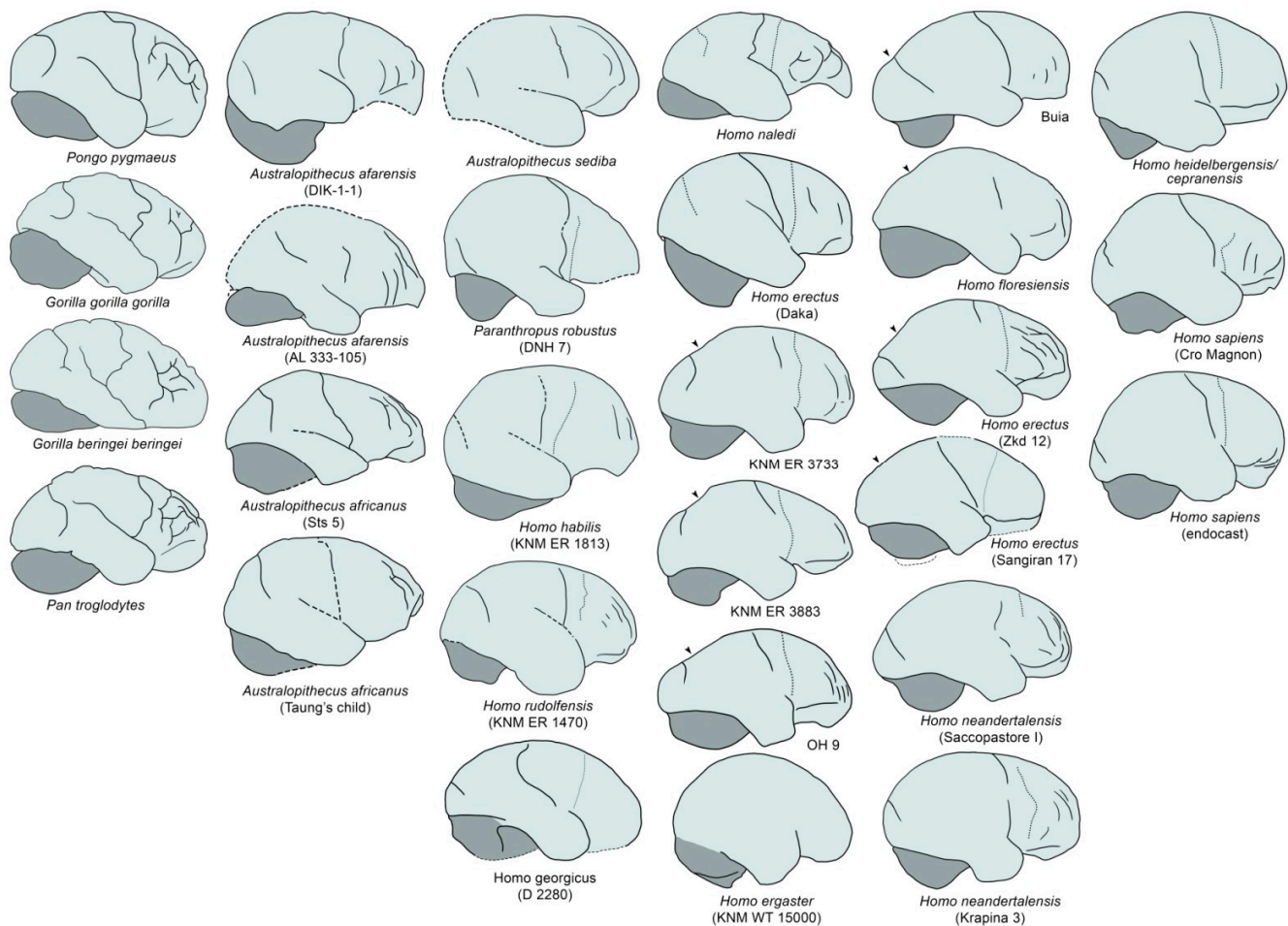


Figure 3 • The morphological dataset. Left column: schemes of the brains of four ape species in right lateral view. All the other columns: schemes of the endocasts of bipedal hominins including *Australopithecus*, *Paranthropus*, and *Homo* species. Dashed lines represent reconstructed portions; dotted lines represent the coronal suture. The black arrowhead indicates the posterodorsal depression observed in the endocasts of *Homo erectus*, *H. floresiensis*, Daka, Buia, KNM ER 3733, and KNM ER 3883. The brains and the endocasts are drawn with the same anteroposterior lengths.

In anterior view, the frontal bec is comparatively longer in *Australopithecus*, *Homo rudolfensis*, *H. georgicus*, Daka, and Buia, whereas it is shorter and difficult to distinguish in *Homo sapiens*, *H. erectus*, and *H. heidelbergensis/cepranensis* (Figure 4). In anterior and posterior views, the outline of the telencephalic hemispheres is uniformly convex and rounded in *Australopithecus afarensis*, *A. africanus*, *Paranthropus*, *Homo rudolfensis*, *H. georgicus*, *H. erectus* (Zkd V), *H. floresiensis*, and *H. heidelbergensis/cepranensis* (Figure 4 and Figure 5). In Sangiran 17, *Homo neandertalensis*, and *Homo sapiens*, a distinctive apex is observed at the dorsolateral corner of the parietal lobe (gray arrowheads in Figure 4 and Figure 5) that gives a more squared shape to the external outline. Moreover, in *Homo sapiens*, the lateral parts of the external outline are straighter and more vertical, giving a more pentagonoid shape to the external outline (Figure 5).

3.2. Descriptions of character states

Based on the above comparisons, we individuated fourteen characters that we then mapped on the reference phylogenies of Figure 1. In the following text, we describe these characters and their variation; the resulting distribution of character states is presented in the taxon x character matrix of Table 2 on a specimen basis.

Character 1. Inclination of outline of posterior portion of endocast and brain posterior to maximum height in lateral view (Figure 3): (0) posterior outline continuously convex; (1) steep inclination of posterior outline and irregular outline with change in inclination of outline individuating a posterodorsal angle of the parietal lobe. A posterodorsal angle is evident in *Pan troglodytes* and several other hominins but is absent in *Pongo* and *Gorilla*.

Character 2. Ventral extension of occipital lobe: (0) absent; (1) present; (2) strong (Figure 3). A ventrally protruded occipital lobe (state 3) is evident in *Homo erectus*, *H. neandertalensis*, and *H. sapiens* (in these species, the posterolateral border of the temporal lobe is visibly concave and the posterior end of the occipital lobe is approximately at the same height as that of the anterior end of the posterolateral border of the temporal lobe, as described in Character 3). In *Pan troglodytes*, *Australopithecus afarensis*, *A. africanus*, *Paranthropus*, *Homo georgicus*, KNM ER 3733, and KNM ER 3883, the occipital lobe shows a slight ventral projection (state 1). In *Pongo*, *Gorilla*, and *Homo naledi*, we do not find any evident ventral protrusion of the occipital lobe. There is apparently no univocal relationship between the ventral protrusion of the occipital lobe and the degree of concavity of the posterolateral border of the temporal lobe, and, for this reason, we coded these two characters separately.

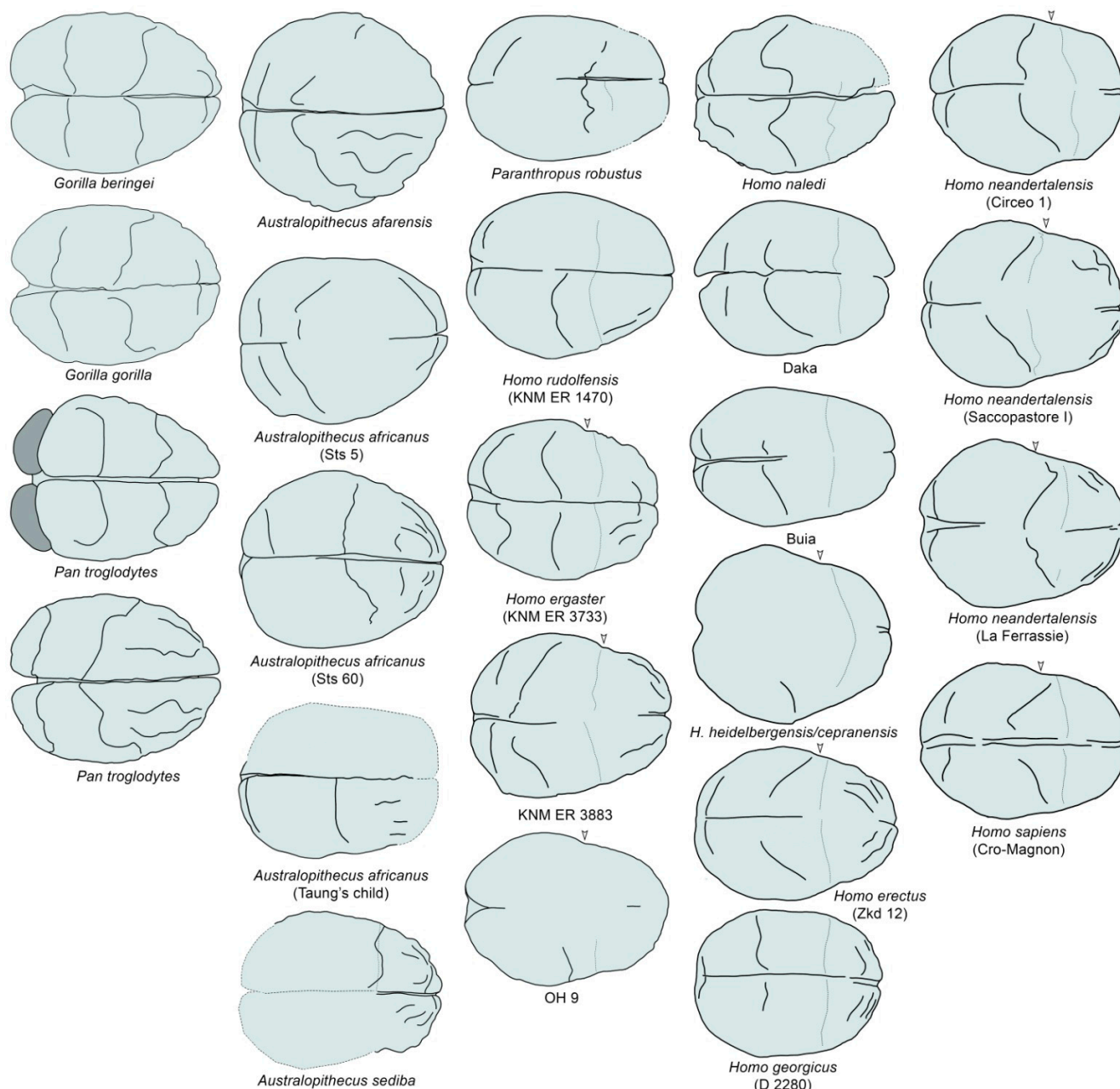


Figure 4 • The morphological dataset. Left column: schemes of the brain of four ape species in dorsal view. Note that one of the chimp brains is shown in posterodorsal view. All the other columns: schemes of the endocasts of bipedal hominins. Dashed lines represent reconstructed portions; dotted lines represent the coronal suture. The white arrowhead indicates the irregular outline of the lateral surface of the endocasts in most *Homo* species.

Character 3. Outline of posterolateral border of temporal lobe in lateral view (**Figure 6A,B**): (0) straight-to-slightly concave with posterior end clearly higher than anterior end; (1) evidently concave with posterior and anterior ends at approximately the same height. In *Pongo*, *Gorilla*, and *Pan*, the outline of the posterolateral border of the temporal lobe is straight-to-slightly concave and the posterior end of the occipital lobe is clearly higher than the anterior end of the border. In **Figure 6E**, the green curve shows this character in the lateral view of the brain of *Pan troglodytes*. The same pattern is observed in *Australopithecus*, *Paranthropus*, *Homo habilis*, *H. rudolfensis*, *H. georgicus*, *H. naledi*, *H. floresiensis*, *H. heidelbergensis/cepranensis*, and Daka (compare images in **Figure 4**). In *Homo erectus*, *H. neandertalensis*, and *H. sapiens*, the posterolateral border is ventrally concave, and the posterior end of the occipital lobe is approximately at the same height as

that of the anterior end of the border (compare specimens in **Figure 3**).

Character 4. Position of parieto-occipital sulcus (**Figure 3** and **Figure 4**): (0) anterior (on an imaginary vertical line crossing the cerebellum approximately at its mid-length); (1) posterior (on an imaginary vertical line crossing the cerebellum in the posterior half); (2) very posterior (on an imaginary vertical line that does not cross the cerebellum, because it is completely posterior to it). The position of the parieto-occipital sulcus is related to the relative development of the occipital lobe and represents an important point in the study of hominid brain evolution as this character can be observed in several endocasts of fossil species. Fundamentally, in *Pongo*, *Gorilla*, and *Pan*, the parieto-occipital sulcus is located anteriorly, and, in all the other hominins in which this structure can be observed, it is positioned significantly posteriorly.

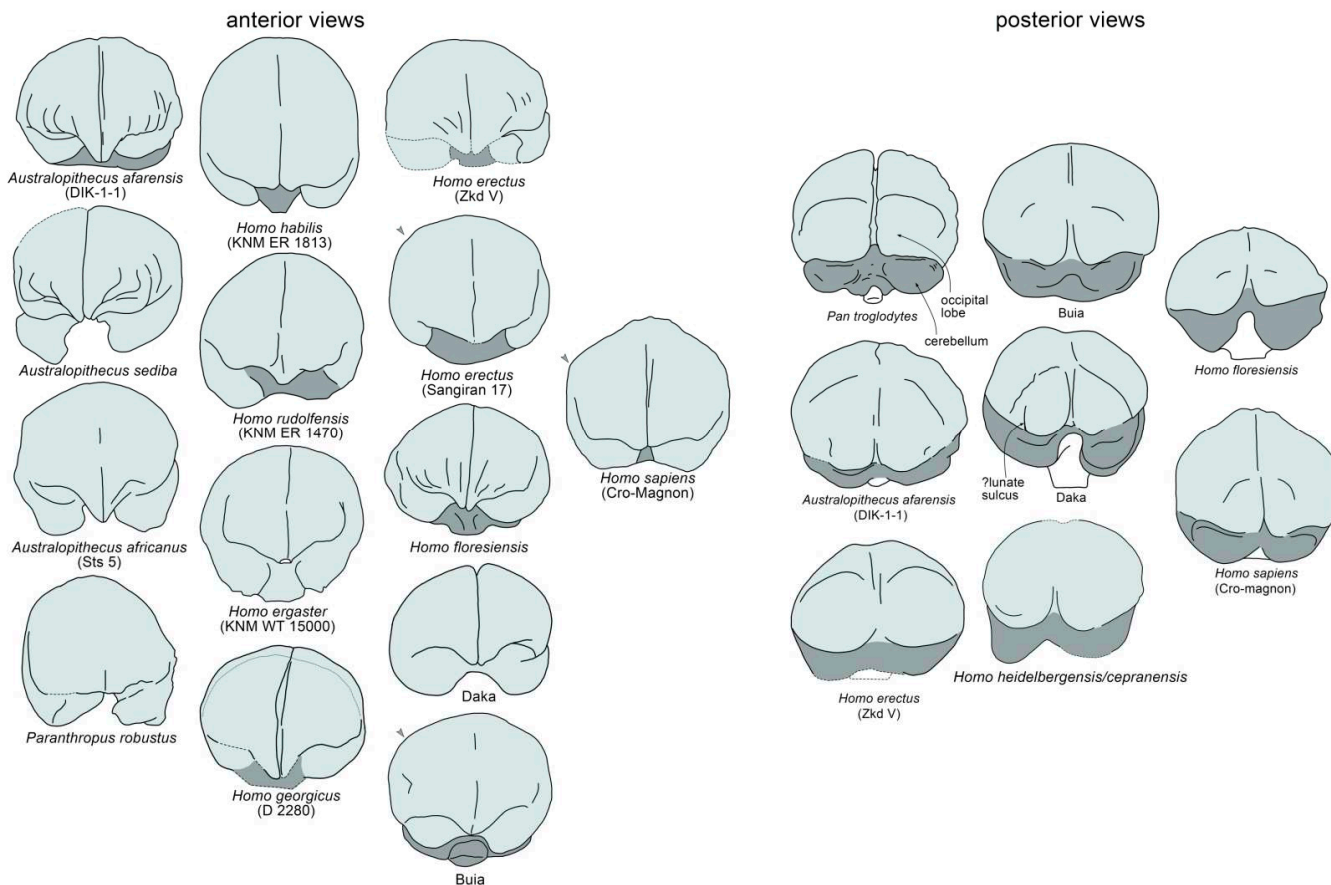


Figure 5 • The morphological dataset. **(Left half):** Endocrania in anterior view. **(Right half):** Endocrania in posterior view. The dotted line represents the trace of the coronal suture; the arrowhead shows the dorsolateral corner observed in the endocrania that gives the endocrania a pentagonoid shape in anterior and posterior views.

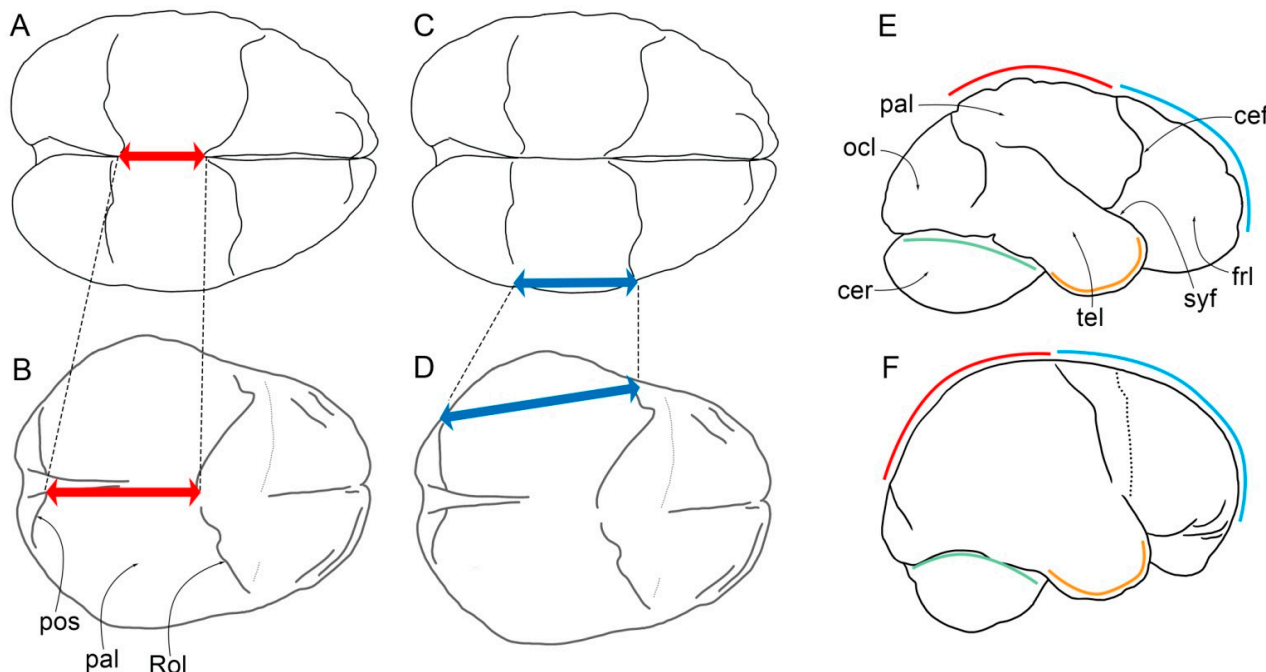


Figure 6 • Comparative plate showing differences between the brain of *Homo sapiens* and that of *Pan troglodytes*. **(A)** A scheme of the chimp brain in dorsal view. **(B)** A scheme of the human brain in dorsal view. **(C)** A scheme of the chimp brain in right lateral view. **(D)** A scheme of the human brain in right lateral view. **(E)** A scheme of the chimp brain in lateral view. **(F)** A scheme of the human brain in lateral view. The red double-arrow headed line indicates the relative medial anteroposterior length of the parietal lobe; the blue double-arrow headed line indicates the relative lateral anteroposterior length of the parietal lobe. The red curve indicates the relative extension of the dorsal edge of the parietal lobe in lateral view; the blue curve indicates the relative roundness and anteroposterior extension of the frontal lobe in lateral view; the green curve indicates the relative degree of ventral concavity of the posteroventral border of the temporal lobe; the yellow curve indicates the relative size of the distal border of the temporal lobe in lateral view.

Character 5. Comparative length of frontal bec in anterior view (**Figure 5**): (0) long; (1) short. Unfortunately, we were able to find only a few examples of endocasts in anterior view, and this limited the extent of our comparison. Nevertheless, we observe the presence of an elongate frontal bec in *Australopithecus afarensis*, *A. sediba*, and *A. africanus*; we also observe an elongate frontal bec in *Homo rudolfensis*, *H. georgicus*, Daka, Buia, and *Homo floresiensis*. Comparatively shorter frontal becs are observed in *Homo habilis*, *H. erectus*, and *H. sapiens*.

Character 6. Width of the base of the frontal bec in anterior view (**Figure 5**): (0) narrow; (1) wide. Narrow frontal becs are observed in *Australopithecus afarensis*, *A. sediba*, *A. africanus*, *Homo rudolfensis*, *H. georgicus*, and *H. floresiensis*. Wider frontal becs are observed in Daka, Buia, *Homo erectus*, and *H. sapiens*. The shape and comparative length of the frontal bec seem uncorrelated (for instance, Daka shows a long but wide frontal bec) and, for this reason, we coded these characters separately.

Character 7. Relative size of anterior portion of temporal lobe: (0) small; (1) large. We observe an evident difference in relative size in the anterior portion of the temporal lobe when comparing *Homo sapiens* and *Pan troglodytes* in **Figure 6A,B**. In that comparison, the distal portion of the temporal lobe of *H. sapiens* is visibly higher than that of *P. troglodytes*, suggesting a corresponding size increase in the temporal lobe of our species with respect to the chimpanzee. We observe a non-homogeneous distribution of this character in our sample as *H. sapiens*, *H. neandertalensis*, *H. heidelbergensis/cepranensis*, *H. ergaster*, *H. rudolfensis*, and possibly *Australopithecus africanus* show comparative size expansion in the anterior portion of the temporal lobe but not the other hominins and great apes.

Character 8. Shape of the central sulcus in lateral view: (0) dorsal end more anterior than ventral end or on the same dorsoventral imaginary line in lateral view; (1) dorsal end more posterior than ventral end in lateral view. The great apes show an anteriorly convex or dorsoventrally straight central sulcus in lateral view (compare images in **Figure 3**; in **Figure 6**, this character is shown in the brain of *Pan troglodytes*) that corresponds to a relative shortness of their frontal lobe. This pattern is also observed in *Australopithecus afarensis*, *A. sediba*, the young *A. africanus* (Taung's child), *Paranthropus*, *Homo habilis*, and *H. rudolfensis*. An anteriorly concave central sulcus is observed in all the other members of the genus *Homo* and in the adult *Australopithecus africanus*, suggesting that this character may show a significant change during ontogeny.

Character 9. Extension of parietal lobe in lateral and dorsal views (**Figure 3** and **Figure 6A,B**): (0) short; (1) long. An elongated parietal lobe is present in all those hominin species in which the central sulcus shows an evident anterior concavity and a posterior displacement of the parieto-occipital sulcus: *Homo sapiens*, *H. neandertalensis*, *H. heidelbergensis/cepranensis*, *H. erectus*, *H. habilis*, and *H. georgicus*. In all the other species of our sample, the parietal lobe is comparatively smaller.

Character 10. Outline of hemispheres in dorsal view (**Figure 4**): (0) uniformly convex; (1) irregular outline. The irregular outline, where present, is due to the lateral protrusion of the temporal lobe observed in *H. sapiens*, *H. neandertalensis*, *H. heidelbergensis/cepranensis*, *H. erectus*, *H. rudolfensis*, *H. ergaster*, KNM ER 3733, and Buia. The irregular shape marks a peculiar size increase in the temporal lobe that could be related to the relative expansion

of the distal border of the temporal lobe described in character 7. We test this hypothesis in the following chapter.

Character 11. Concavity in the dorsal border of the cerebral hemisphere in lateral view in posterior portion of parietal lobe (**Figure 3**, black arrowhead): (0) absent; (1) present. We observe this concavity in KNM ER 3733, KNM ER 3883, OH9, Buia, *Homo floresiensis*, and *Homo erectus*. In the other specimens, the concavity is absent.

Character 12. Outline of posterodorsal portion of the frontal lobe in lateral view: (0) straight-to-slightly convex; (1) uniformly convex and round. The evident roundness of the frontal lobe in lateral view is observed in *Australopithecus sediba*, in all the members of the genus *Homo* but *H. naledi*, KNM ER 3883, and, interestingly, in the Taung child but not in Sts 5.

Character 13. Orientation of medial portion of central sulcus in dorsal view: (0) projects transversely; (1) shows an anteriorly concave outline; (2) projects anteriorly. In the great apes, the central sulcus projects transversely in dorsal view and shows an anteriorly convex outline, and the same pattern is observed in the Taung child, *Australopithecus sediba*, and *Homo georgicus*. In the other australopithecines, *Paranthropus*, and the other species of *Homo* but *H. georgicus*, the shape of the central sulcus is different. In *Australopithecus afarensis*, the adult *A. africanus* (Sts 5), KNM ER 3883, Daka, Buia, *Homo erectus*, *H. neandertalensis*, and *H. sapiens*, the central sulcus projects anteriorly in dorsal view in a sharp manner.

Character 14. Comparative height of cerebral hemispheres in lateral view: (0) low; (1) high. We find that in *Homo sapiens*, *H. heidelbergensis/cepranensis*, *H. habilis*, and *Paranthropus robustus*, the cerebral hemispheres are comparatively higher than in the other specimens examined. This character is unlikely to provide a phylogenetic signal given its disparate distribution, but we test this hypothesis in the next paragraph.

3.3. Character mapping at ancestral nodes

The distributions of the fourteen character states described above on the phylogeny of **Figure 1** are shown in **Figure 7**, **Figure 8** and **Figure 9**. The maximum likelihood algorithm implemented in MESQUITE found that the posterior outline of the cerebral hemispheres in lateral view is not uniformly convex (character 1) and a ventral protrusion of the occipital lobe (character 2) originated within apes as these characters are present in all hominids with the exclusion of *Pongo* and *Gorilla*. The only character that can be related to the origin of bipedal hominids is the posteroventral placement of the parieto-occipital sulcus (character 4) that is present in all the australopithecines, *Paranthropus*, and *Homo*. However, judging from our maps, the distribution of this character state in the present sample is not unambiguous and the character could be the result of parallel evolution in australopithecines and *Homo*. There are no evident apomorphic characters able to support the eventual monophyly of *Australopithecus*; therefore, our paleoneurological work confirms the paraphyly of this hominid genus; however, given that the australopithecine sample size is very limited and that some of the analyzed australopithecine endocasts are incomplete, we suggest that further work is necessary to provide a robust morphological support to a hypothesis of paraphyly of *Australopithecus*.

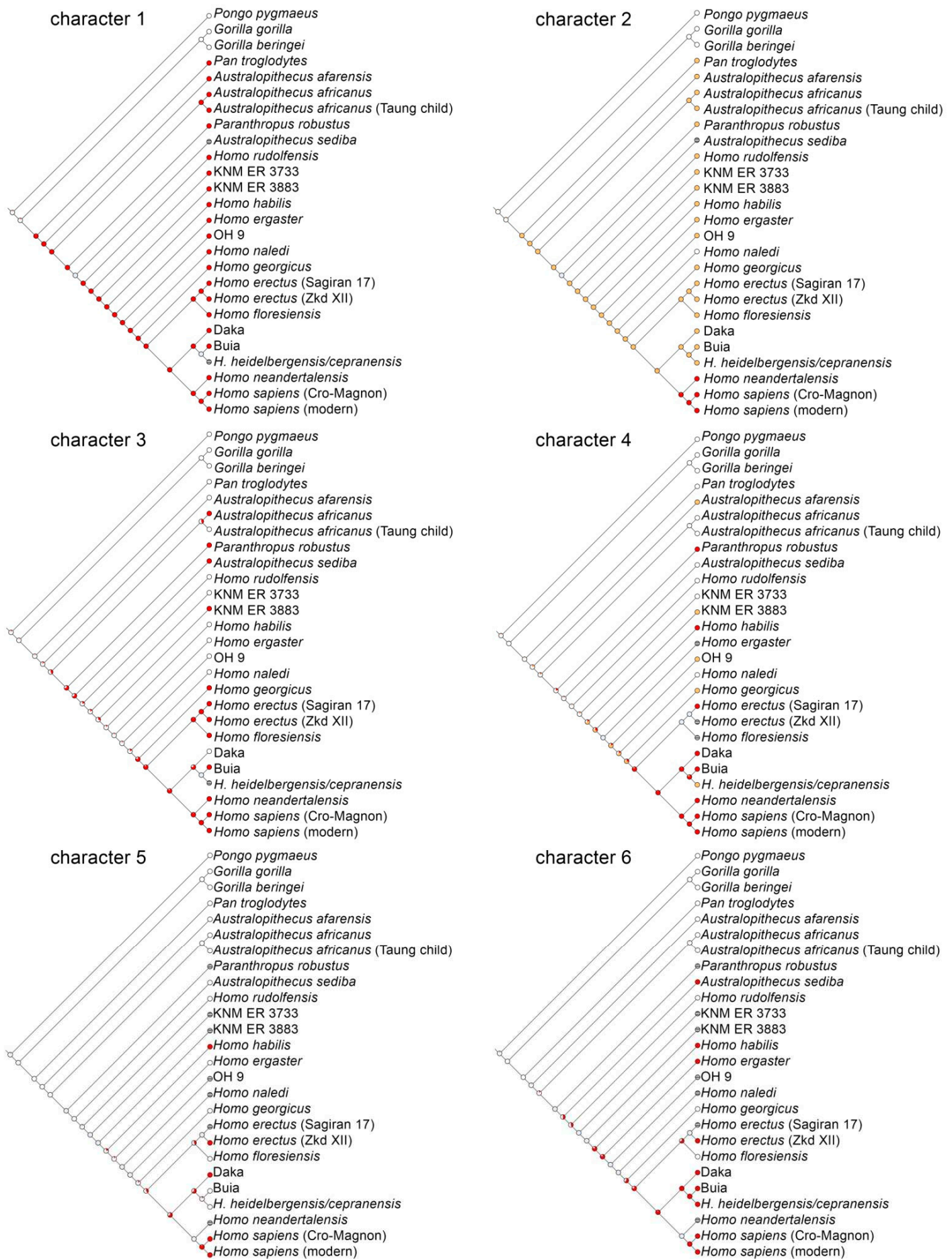


Figure 7 • The distribution of character states 1–6 on the reference phylogeny based on maximum likelihood. White circles represent state 0, orange circles represent state 1, and red circles represent state 2.

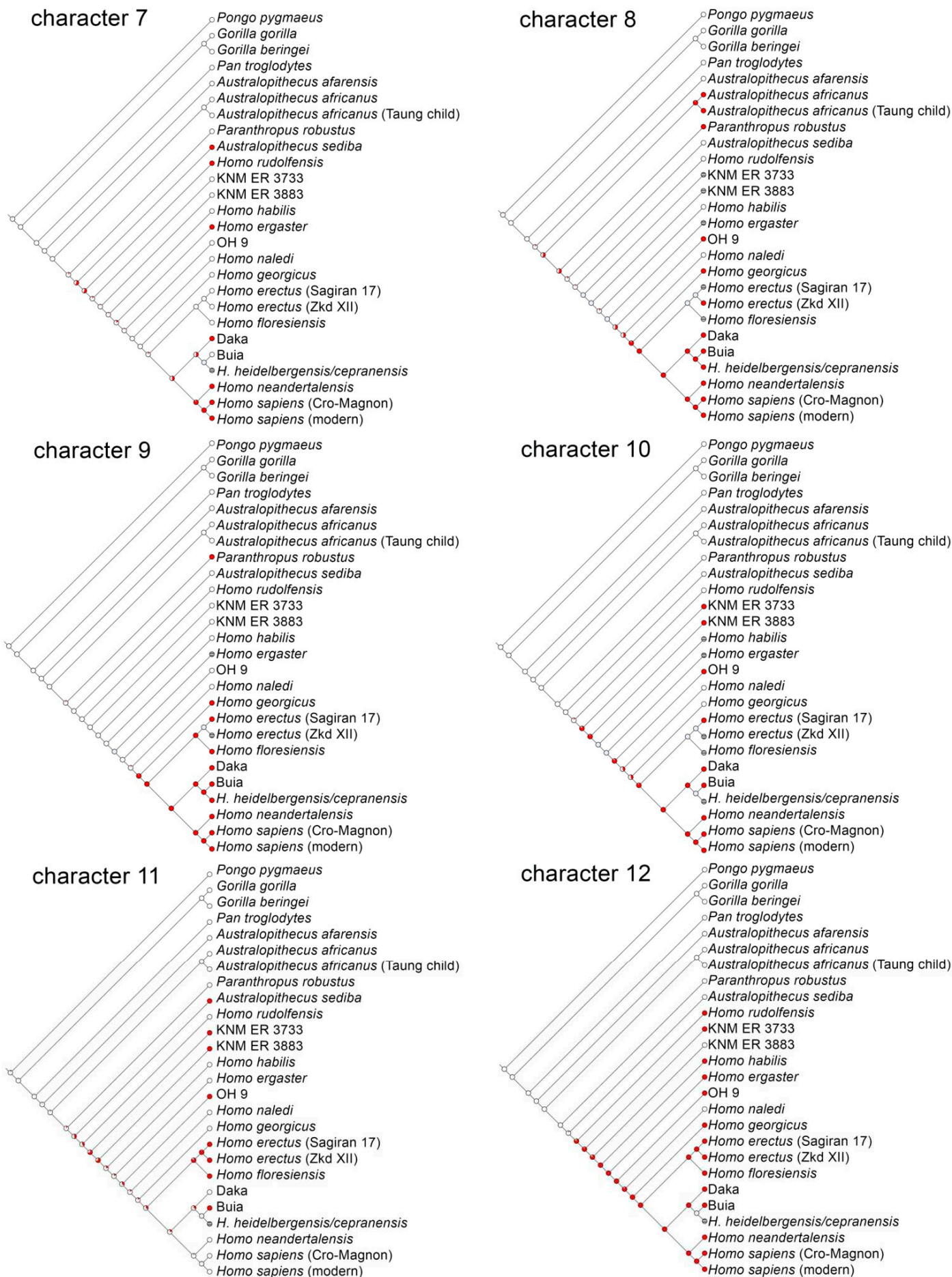


Figure 8 • The distribution of character states 7–12 on the reference phylogeny based on maximum likelihood. White circles represent state 0, orange circles represent state 1, red circles represent state 2, and gray circles represent states that could not be inferred.

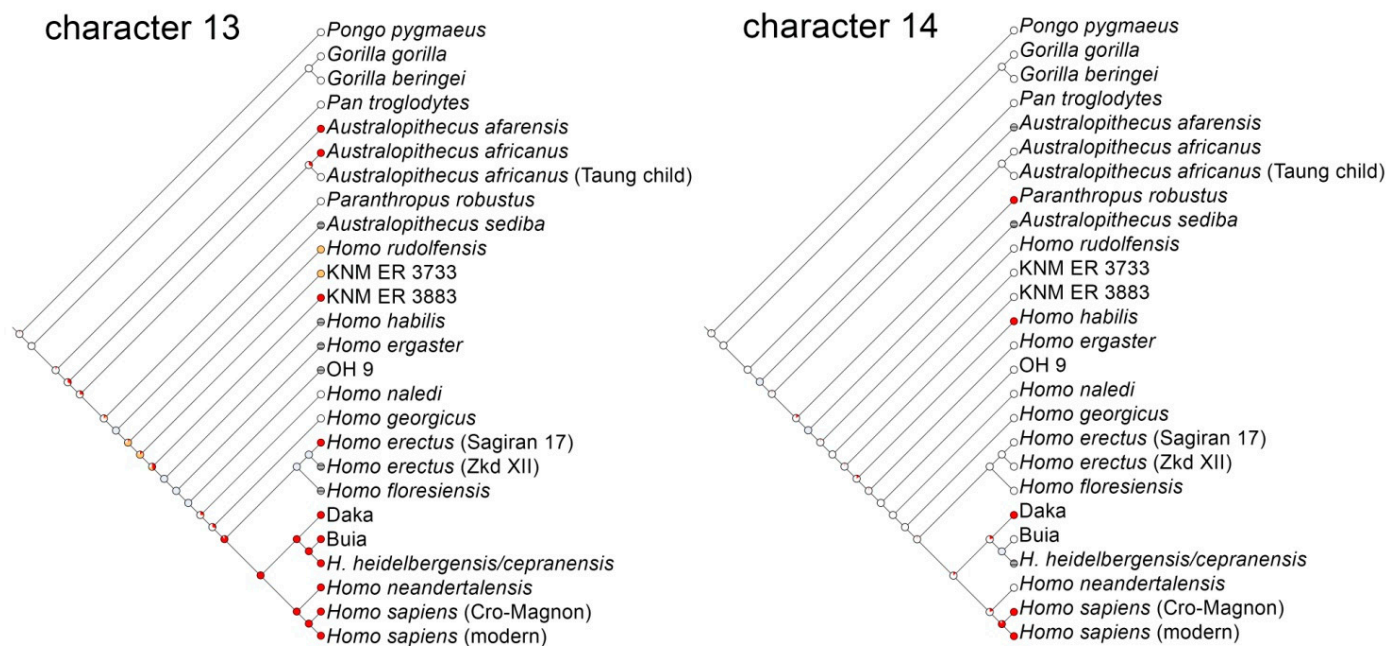


Figure 9 • The distribution of character states 13–14 on the reference phylogeny based on maximum likelihood. White circles represent state 0, orange circles represent state 1, red circles represent state 2, and gray circles represent states that could not be inferred.

We observe different character states within *Australopithecus africanus* by comparing the Taung child with Sts 5; in particular, characters 3 (outline of posterolateral border of temporal lobe) and 13 (orientation of medial fissure in dorsal view) suggest that morphological changes occurring during the late ontogeny of *Australopithecus africanus* may be responsible for differences observed in these specimens. Character 13 is related to the shape of the central sulcus which is related to the expansion of the primary sensory and the primary motor cortices. Here, we suggest that the adult shape and, by implication, the adult extension of these cortices were reached after a postnatal ontogenetic transformation process in *Australopithecus africanus*.

We did not find any evident apomorphic characters supporting the sister group relationship of *Paranthropus* and the clade formed by *Australopithecus sediba* + *Homo*. Rather, we found that the sister group relationship of *Australopithecus sediba* and *Homo* is supported by characters 6 (wide base of frontal bec) and 7 (comparatively large size of the anterior portion of the temporal lobe).

The earliest members of the genus *Homo* show a change in the orientation of the central sulcus in dorsal view (character 13); in particular, in *Homo rudolfensis* and KNM ER 3733, we observe that the central sulcus shows an anterior concavity in dorsal view differing from that of australopithecines and apes that project transversely. However, this character cannot be used to support the monophyly of *Homo*, because in later species (like *Homo erectus*, *H. sapiens*, *H. neandertalensis*, etc.), we observe a reversal of this character to a shape already observed in the adult *Australopithecus africanus* and *A. afarensis* (central sulcus projects anteriorly in a sharp manner).

Paleoneurological characters support the monophyly of later *Homo* species. A wider frontal bec (character 6), a remarkable anteroposterior elongation of the parietal lobe (character 9), and a sharp anterior projection of the central sulcus (character 13) are shared by a clade including Buia, *Homo georgicus*, *H. erectus*, *H.*

heidelbergensis/cepranensis, *H. neandertalensis*, and *H. sapiens*. Character 10 (sigmoid outline of cerebral hemispheres in dorsal view) supports the sister group relationship of OH9 and a clade including all the other *Homo* species with the exclusion of *H. rudolfensis*, *H. habilis*, KNM ER 3733, and KNM ER 3883. Characters 2 (strong ventral extension of occipital lobe) and 7 (large distal portion of temporal lobe) support the monophyly of *Homo neandertalensis* and *Homo sapiens*.

4. Discussion

The evolution of the human brain represents the main avenue of scientific research for obvious reasons. Several comparative morphological works have been published on this topic in the last two decades (e.g., [3, 35, 48, 49]) together with numerous articles about encephalization and other quantitative indices able to describe the increase in brain volume typical of our species with respect to the other mammals (e.g., [37, 39, 50]). Studies on cranial endocasts provide fundamental evidence about the morphology of the brain covered by the meninges of extinct human species with the well-known limits of this kind of research (e.g., [51]). As difficult as they are to interpret, endocasts still represent unavoidable sources of morphological data, sources that are now supplemented by the increasing number of three-dimensional renderings of virtual endocasts obtained through CT scans. In the end, both natural and virtual endocasts provide morphological data about aspects of brain shape and size that would be impossible to obtain in other ways for extinct species.

We compared several endocasts of apes and bipedal hominins to obtain a synthetic view of the evolutionary changes that occurred in the gross morphology of the brain in the phylogenetic lineage leading to the modern humans. Given that we are aware of the limits of the morphological data presented by endocasts, we limited our analysis to only a few evident characters able to represent the main transformations of the hominid brains over the last 15 million years.

The comparative analysis allowed us to identify and describe fourteen morphological characters in about 24 operational taxonomic units including four ape species and twenty bipedal hominins including *Australopithecus*, *Paranthropus*, and *Homo*. We then mapped the character states onto a reference phylogeny obtained from a detailed study of the literature and reconstructed endocast characters at ancestral nodes and, in so doing, we inferred a transformational path of the brain within Hominidae.

Our results agree with some previous works in that we observed that the posteroventral placement of the parieto-occipital sulcus is one of the earliest steps of brain modification that occurred at the transition between *Pan* and *Australopithecus* (e.g., [26]). We observed that in lateral view, the roundness of the brain increased in two separate phases: (1) at the transition between *Pan* and *Australopithecus*, and (2) at the transition between *Australopithecus* and *Homo*. We observed that a peculiar enlargement of the parietal lobe occurred in the clade formed by *Homo georgicus*, *H. sapiens*, their common ancestor, and all the descendants of this ancestor, and that a marked enlargement of the distal portion of the temporal lobe occurred in the clade formed by *Homo sapiens*+*H. neandertalensis*. A synthesis of these transformations is presented in **Figure 10**.

We can find a limited number of key transformations in the wide variation observed in the sample of endocasts analyzed in the present paper; those transformations are listed in the previous chapter and shown in **Figure 10**. Interestingly, these key changes were about the evolutionary history of specific portions of the brains in different times of human evolution. Apparently, the first important step in hominin brain evolution was the reorganization of the occipital lobe by the ventromedial placement of the parieto-occipital sulcus; this character probably has something to do with (1) the anteroposterior expansion of the parietal lobe, (2) a reorganization of the visual cortex at the transition between *Pan* and *Australopithecus*, and (3) a redistribution of weight within the cranial cavity in response to the origin of bipedalism. Unfortunately, there is no evidence of the endocast morphology of earlier and more primitive bipedal hominins like *Orrorin*, *Ardipithecus*, *Sahelanthropus*, *Kenyanthropus*, *Australopithecus ramidus*, *Au. anamensis*, and *Au. garhi*. For this reason, we cannot know exactly when the parieto-occipital sulcus moved posteroventrally; we can state that this transformation occurred at the divergence of *Pan* and *Australopithecus* between the latest Tortonian and the earliest Piacenzian.

After that phase, we observe a massive adaptive radiation of early *Homo* species including *H. rudolfensis*, *H. habilis*, *H. ergaster*, KNM ER 3733, KNM ER 3883, *Homo naledi*, and *Homo georgicus* in a time interval of about 600 ka between about 2.4 and 1.8 Ma. During this phase, several transformations occurred in the brain of bipedal hominins including an increased roundness of the frontal lobe and new orientations of the central sulcus (reasonably related to a reorganization of the primary motor cortex). While the increased roundness could be related to a reorganization and size increase of the premotor cortex, interestingly, this morphological and functional change is not in good agreement with the archeological record as stone tools begin to become common, in the stratigraphic record, starting from more than 3 million years ago [52]; their origin, therefore, pre-dates the modifications of the primary motor cortex and of the premotor cortex. Whether the hypothesis that australopithecines were the earliest stone tool

manufacturer is accepted or not [53], it must be accepted that stone tool manufacture was possible without a marked modification of the motor cortex with respect to the great apes. There are several interesting implications following this logical reasoning that take into consideration the ability of extant apes to prepare wood and leaf instruments (e.g., [54]) and to make stone tools [55].

Three transformations occurred in the hominin brain in the lineage providing the common ancestor of *Homo georgicus*, *H. erectus*, *H. floresiensis*, *H. neandertalensis*, *H. sapiens*, *H. heidelbergensis/cepranensis*, Daka, and Buia. These transformations include an anteroposterior expansion of the parietal lobe, a new orientation of the central sulcus, and a widening of the frontal bec. The first and the second transformations could be put into relation with changes in size and shape of the primary sensory cortex and with peculiar changes in the sizes of areas located in the parietal lobe. These include areas 7 and 39 that are collectively referred to as posterior associative areas and have to do with attention mechanisms and the associative processing of sensorial stimuli (e.g., [56–58]). More detailed analyses could help in understanding the exact amount of anteroposterior expansion of the parietal lobe in these species and the results could be used to test eventual associations between the relative size of the parietal areas and the origin of the Acheulean technology [56]. Such a test is outside the scope of the present paper.

The difference in size between the prefrontal cortices of *H. neandertalensis* and *H. sapiens* is not clearly detectable in the fossil data. Holloway, at first [59], tried to show that Neanderthals had a smaller frontal lobe than modern humans, but changed his mind later [60]. A refined geometric morphometrics analysis [61] could not find a significant difference in the roundness of the forebrain. More recently, ref. [62] found that the two largest-brained species have both experienced a non-allometric increase in the frontal width. Still, Neanderthals have the most apparent latero-lateral frontal enlargement, even when compared with *H. sapiens*.

A subtle or no difference in frontal lobe size and shape emerges when morphometric computational anatomy (surface-displacement-based morphometry, d-bm) is used to compare the surface morphology and size between NT and MH in the frontal region [45]. Conversely, endocast morphometry and d-bm show significant morphological differences in the cerebellar, parietal, occipital, and medial temporal regions.

Some studies [63, 64], on the other hand, seem to agree that Neanderthals had a larger occipital region, likely due to a more developed visual cortex. Considering that the proportion of the parieto-occipital cortical block remains relatively constant across apes and humans [65], a comparatively larger occipital cortex would likely be accompanied by a relatively reduced parietal cortex.

García-Taberner et al. [66] observed (a) a deviation in the occipital pole fossa from the mid-sagittal plane in *Homo neandertalensis*, (b) a deviation in the occipital portion of the brain, and (c) an inclination of the supra- and infracalcarine fossae compared with *H. sapiens*, which might suggest differentiated patterns between these two species.

From our analysis, the brains of modern humans and Neanderthals show changes in the relative size of the distal portion of the temporal lobe and a marked ventral protrusion of the occipital lobe, giving the posterolateral border of the temporal lobe a ventrally concave outline. It is not to be excluded that these transformations provided

increased capacity for memory and emotive control. In particular, on the left side, the enlargement of the temporal lobe is to be related to an increase in memory and language-related capacities, and, on the right side, to capacities required for improvement in emotional functions. A functional asymmetry in the human brain is reflected to some extent in morphological (and morphometric) asymmetry. These subtle differences can be found at both macroscopic and microscopic levels (distribution of nerve cells, connectivity, and neurochemistry). In a comparative context, however, endocranial asymmetry is not a human prerogative, but it is shared with all the great apes. This is true for some of the asymmetry patterns previously described as prerogative on *Homo*: not only humans, but also chimpanzees, gorillas, and orangutans exhibit the asymmetry pattern previously described as uniquely human. Specifically, the left occipital lobe, the right frontal lobe, and the right temporal pole and right cerebellar lobe project more prominently toward their contralateral counterparts. On the other hand, another study [67] was able to detect a much more variable asymmetry compared to other great apes with high species-specific variation. A recent study [68] does not appear to support the hypothesis [69], which, based on MRI data, suggested that modern humans possess a right temporal lobe that is not only absolutely but also relatively larger in proportion to the right hemispheric volume when compared to that of other anthropoid apes. In any case, we must hypothesize that a positive association between brain transformations and the complexity of stone tool assemblages must be hypothesized as *H. neandertalensis* and early *H. sapiens* are related to the spreading

of the Middle Paleolithic stone tool technology, to burial-related ritualistic behaviors, and to the manufacture of ornamental items (e.g., [70]).

The lunate sulcus (LS) marks the front boundary of the primary visual cortex (V1) and its position in the occipital lobe has been used to assess evolutionary brain changes. In apes, it is positioned more anteriorly, while in humans, it is more posterior. In Australopithecines, debate exists over whether the LS had shifted posteriorly, indicating early brain reorganization, or remained in an ape-like anterior position. Researchers like Falk [71] argue that it remained anterior, suggesting a brain size increase came first, while Holloway ([72] and the literature therein) contends that it was already posterior, implying that reorganization occurred without size change.

It is important to note that the controversy surrounding the position of the lunate sulcus extends beyond the paleoneurology of the human clade and encompasses extant species. In general, the position of the lunate sulcus appears to be significantly more variable in humans than in apes and does not consistently demarcate the anterior boundary of the occipital lobe. Intriguingly, several scholars have questioned whether the lunate sulcus observed in anthropoid apes is truly homologous to that found in humans [73]. In any case, the morphology of LS appears variable in humans because of substantial brain enlargement and reorganization, with a functional dissociation from the visual cortex [74].

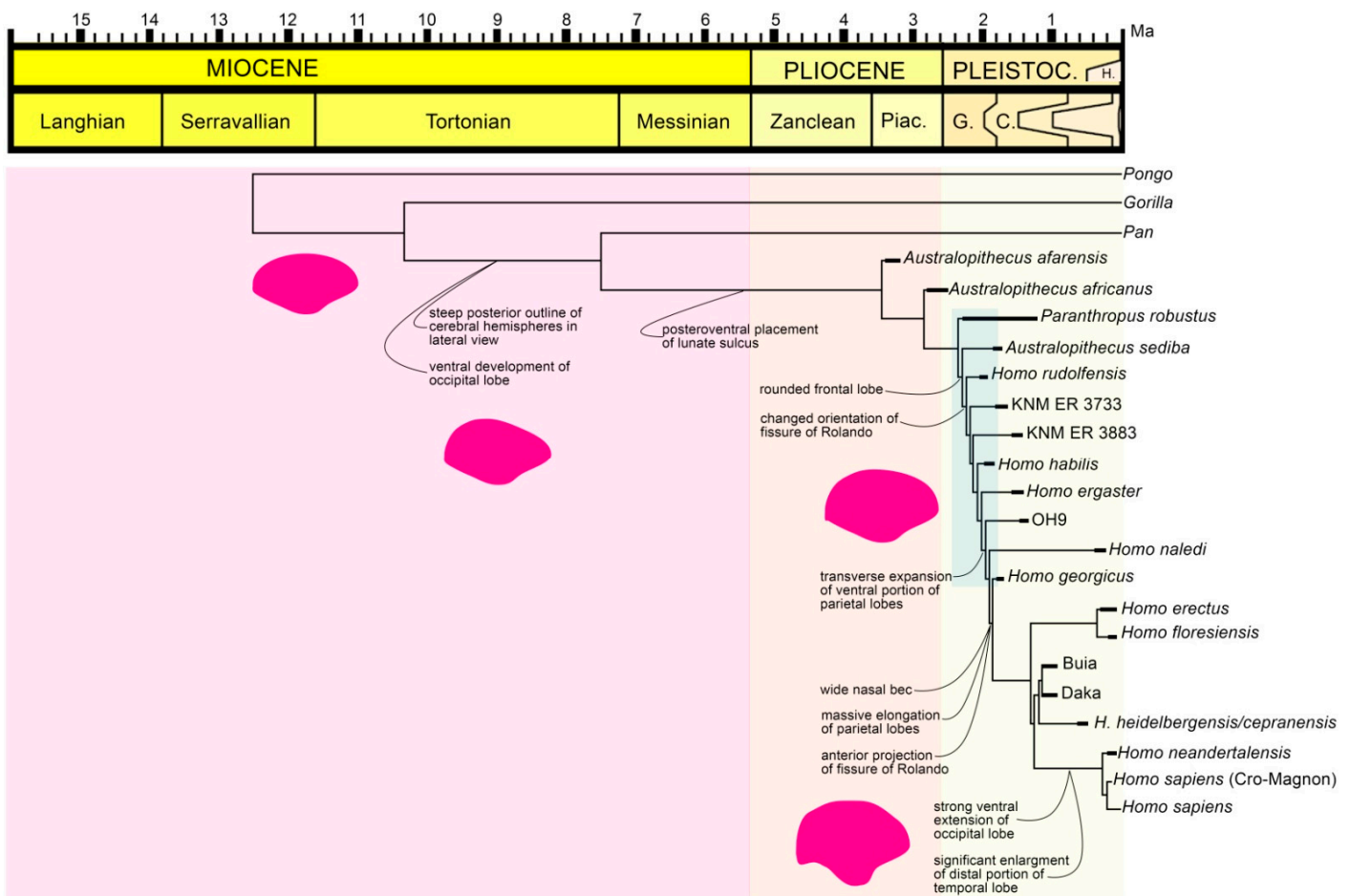


Figure 10 • Synthetic representation of the main morphological transformations of the hominid brain in the last 15 million years. The fuchsia silhouettes represent schemes of brains showing the principal morphological characters studied in the present paper. Caption: C., Calabrian; G., Gelasian; H., Holocene; PLEISTOC., Pleistocene. The light blue rectangle indicates the Early Pleistocene *Homo* radiation.

5. Conclusions

In the end, our work provides a framework about the evolution of the gross morphology of the hominid brain. We identified a limited number of morphological changes that occurred in the hominin brain since the chimp–australopithecine divergence, showing the origin of key characters in determinate periods of hominid evolution. We confirm previous works about mosaic evolution of the brain surface in hominins and show key transformations possibly related to functional outputs that can be tested against the archeological record of hominin behavior. The limits of our work are in the reduced number of endocasts used in our analyses and in the quality of the endocast preservation that can be insufficient to warrant observation of anatomical details. The inclusion of additional specimens to our dataset will refine our conclusions and help in deciphering the side evolutionary trends observed in extinct hominin species.

Acknowledgments

The authors sincerely thank Dean Falk who provided the literature.

Funding

This research received no external funding.

Author contributions

Conceptualization, M.B. and G.T.; methodology, M.B.; software, M.B.; validation, M.B. and G.T.; formal analysis, M.B. and G.T.; investigation, M.B.; resources, M.B. and G.T.; data curation, G.T.; writing—original draft preparation, M.B.; writing—review and editing, M.B. and G.T.; visualization, M.B.; supervision, M.B. and G.T.; project administration, M.B. and G.T. All authors have read and agreed to the published version of the manuscript.

Conflict of interest

The authors declare no conflicts of interest.

Data availability statement

Data supporting these findings are available within the article, at <https://doi.org/10.20935/AcadBiol7710>, or upon request.

Institutional review board statement

Not applicable.

Informed consent statement

Not applicable.

Additional information

Received: 2025-01-17

Accepted: 2025-05-06

Published: 2025-05-23

Academia Biology papers should be cited as *Academia Biology* 2025, ISSN 2837-4010, <https://doi.org/10.20935/AcadBiol7710>. The journal's official abbreviation is *Acad. Biol.*

Publisher's note

Academia.edu Journals stays neutral with regard to jurisdictional claims in published maps and institutional affiliations. All claims expressed in this article are solely those of the authors and do not necessarily represent those of their affiliated organizations, or those of the publisher, the editors and the reviewers. Any product that may be evaluated in this article, or claim that may be made by its manufacturer, is not guaranteed or endorsed by the publisher.

Copyright

© 2025 copyright by the authors. This article is an open access article distributed under the terms and conditions of the Creative Commons Attribution (CC BY) license (<https://creativecommons.org/licenses/by/4.0/>).

References

1. Almécija S, Hammond AS, Thompson NE, Pugh KD, Moyà-Solà S, Alba DM. Fossil apes and human evolution. *Science*. 2021;372:eabb4363. doi: 10.1126/science.abb4363
2. Jerison HJ. Evolution of the brain and intelligence. New York: Academic Press; 1973.
3. Tartarelli G, Bisconti M. Trajectories and constraints in brain evolution in primates and cetaceans. *Hum Evol*. 2006;21:275–87. doi: 10.1007/s11598-006-9027-4
4. Bisconti M, Damarco P, Tartarelli G, Pavia M, Carnevale G. A natural endocast of an early Miocene odontocete and its implications in cetacean brain evolution. *J Comp Neurol*. 2021;529:1198–227. doi: 10.1002/cne.25015
5. Marino L, McShea DW, Uhen MD. Origin and evolution of large brains in toothed whales. *Anat Rec A Discov Mol Cell Evol Biol*. 2004;281:1247–55. doi: 10.1002/ar.a.20128
6. Bruner E, Ogihara N, Tanabe HC. Digital endocasts. From skulls to brains. Tokyo: Springer; 2018.
7. Lautenschlager S. Reconstructing the past: methods and techniques for the digital restoration of fossils. *R Soc Open Sci*. 2016;3:160342. doi: 10.1098/rsos.160342
8. Bruner E, Bondioli L, Coppa A, Frayer DW, Holloway RL, Libsekal Y, et al. The endocast of the one-million-year-old human cranium from Buia (UA 31), Danakil Eritrea. *Am J Phys Anthr*. 2016;160:458–68. doi: 10.1002/ajpa.22983
9. Grimaud-Hervé D, Lordkipanidze D. The fossil hominids' brain of Dmanisi: D 2280 and D 2282. In: Broadfield D, Yuan M, Schick K, Toth N, editors. The human brain evolving: paleoneurological studies in honor of Ralph L Holloway. Vol.

4. Gosport (IN): Stone Age Institute Publication Series; 2010. p. 59–82.
10. Beaudet A, Clarke RJ, Bruxelles L, Carlson KJ, Crompton R, de Beer F, et al. The bony labyrinth of StW 573 (“Little Foot”): implications for early hominin evolution and paleobiology. *J Hum Evol.* 2019;127:67–80. doi: 10.1016/j.jhevol.2018.12.002
11. Conde-Valverde M, Martínez I, Quam RM, Bonmatí A, Lorenzo C, Velez AD, et al. The coclea of the Sima de los Huesos hominins (Sierra de Atapuerca, Spain): new insights into cochlear evolution in the genus *Homo*. *J Hum Evol.* 2019;136:102641. doi: 10.1016/j.jhevol.2019.102641
12. Kaas JH. The evolution of brains from early mammals to humans. *Wiley Interdiscip Rev Cogn Sci.* 2013;4:33–45. doi: 10.1002/wcs.1206
13. Amunts K, Zilles K. Architectonic mapping of the human brain beyond Brodmann. *Neuron.* 2015;88:1086–107. doi: 10.1016/j.neuron.2015.12.001
14. Balzeau A, Grimaud-Hervé D, Détroit F, Holloway RL, Combès B, Prima S. First description of the Cro-Magnon 1 endocast and study of brain variation and evolution in anatomically modern *Homo sapiens*. *Bull Mém Soc Anthropol Paris.* 2013;25:1–18. doi: 10.1007/s13219-012-0069-z
15. Mongle CS, Strait DS, Grine FE. An updated analysis of hominin phylogeny with an emphasis on re-evaluating the phylogenetic relationships of *Australopithecus sediba*. *J Hum Evol.* 2023;175:103311. doi: 10.1016/j.jhevol.2022.103311
16. Pozzi L, Hodgson JA, Burrell AS, Sterner KN, Raam RL, Disotell TR. Primate phylogenetic relationships and divergence dates inferred from complete mitochondrial genomes. *Mol Phylogenet Evol.* 2014;75:165–83. doi: 10.1016/j.ympev.2014.02.023
17. Püchel HP, Bertrand OC, O’Reilly JE, Bobe R, Püchel TA. Divergence-time estimates for hominins provide insight into encephalization and body mass trends in human evolution. *Nat Ecol Evol.* 2021;5:808–19. doi: 10.1038/s41559-021-01431-1
18. Feng X, Lu D, Gao F, Fang Q, Feng Y, Huang X, et al. The phylogenetic position of the Yunxian cranium elucidates the origin of dragon man and the denisovans. *BioRxiv.* 2023. doi: 10.1101/2024.05.16.594603
19. Miller IA, Barton RA, Numm CL. Quantitative uniqueness of human brain evolution revealed through phylogenetic comparative analysis. *eLife.* 2019;8:e41250. doi: 10.7554/eLife.41250
20. Zeitoun V, Barriel V, Widianto H. Phylogenetic analysis of the calvaria of *Homo floresiensis*. *CR Palevol.* 2016;15:555–68. doi: 10.1016/j.crpv.2015.12.002
21. Mounier A, Caparros M. The phylogenetic status of *Homo heidelbergensis*—a cladistic study of middle pleistocene hominins. *BMSAP.* 2015;27:110–34. doi: 10.1007/s13219-015-0127-4
22. Mallegni F, Carnieri E, Bisconti M, Tartarelli G, Ricci S, Segre A. *Homo cepranensis sp. nov.* and the evolution of African-European Middle Pleistocene hominids. *CR Palevol.* 2003;2:153–9. doi: 10.1016/S1631-0683(03)00015-0
23. Shellshear JL. The arteries of the brain of the Orang-Utan. *J Anat.* 1927;61(Pt 2):167–97.
24. Navarrete AF, Blezer ELA, Pagnotta M, de Viet ESM, Todorov OS, Lindenfors P, et al. Primate brain anatomy: new volumetric MRI measurements for neuroanatomical studies. *Brain Behav Evol.* 2018;91(2):109–117. doi: 10.1159/000488136
25. Sherwood CC, Cranfield MR, Mehlman PT, Lilly AA, Garbe JAL, Whittier CA, et al. Brain structure variation in great apes, with attention to the Mountain Gorilla (*Gorilla beringei beringei*). *Am J Primatol.* 2004;63:149–61. doi: 10.1002/ajp.20048
26. Gunz P, Neubauer S, Falk D, Tafforeau P, Le Cabec A, Smith TM, et al. *Australopithecus afarensis* endocasts suggest ape-like brain organization and prolonged brain growth. *Sci Adv.* 2020;6:eaaz4729. doi: 10.1126/sciadv.aaz4729
27. Holloway RL, Broadfield DC, Yuan MS. Morphology and histology of chimpanzee primary visual striate cortex indicate that brain reorganization predated brain expansion in early hominid evolution. *Anat Rec.* 2003;273:594–602. doi: 10.1002/ar.a.10071
28. Holloway RL, Sherwood CC, Hof PR, Rilling JK. Evolution of the brain, in humans—paleoneurology. Specializations in a comparative perspective. In: Binder MD, Hirokawa N, Windhorst U, editors. *Encyclopedia of neuroscience*. Berlin: Springer; 2009. doi: 10.1007/978-3-540-29678-2_3153
29. Falk D. The natural endocast of Taung (*Australopithecus africanus*): insights from the unpublished papers of Raymond Arthur Dart. *Yearb Phys Anthropol.* 2009;52:49–65. doi: 10.1002/ajpa.21184
30. Holloway RL, Broadfield DC, Carlson KJ. New high-resolution computed tomography data of the Taung partial cranium and endocast and their bearing on metopism and hominin brain evolution. *Proc Natl Acad Sci USA.* 2014;111:13022–27. doi: 10.1073/pnas.1402905111
31. Beaudet A, Dumoncel J, de Beer F, Durrleman S, Gilissen E, Oettlé G, et al. The endocranial shape of *Australopithecus africanus*: surface analysis of the endocasts of Sts 5 and Sts 60. *J Anat.* 2018;232:296–303. doi: 10.1111/joa.12745
32. Neubauer S, Gunz P, Weber GW, Hublin J-J. Endocranial volume of *Australopithecus africanus*: new CT-based estimates and the effects of missing data and small sample size. *J Hum Evol.* 2012;62:498–510. doi: 10.1016/j.jhevol.2012.01.005
33. Carlson KJ, Stout D, Jashashvili T, de Ruiter DJ, Tafforeau P, Carlson K, et al. The endocast of MH1, *Australopithecus sediba*. *Science.* 2011;333:1402–7. doi: 10.1126/science.1203922

34. Falk D, Marom A. The DNH 7 endocast of *Paranthropus robustus* from Drimolen, South Africa: reconsidering the functional significance of an enlarged occipital-marginal (O/M) sinus system in robust australopithecines. *Am J Biol Anthropol.* 2024;185:e25010. doi: 10.1002/ajpa.25010
35. Holloway RL. The evolution of the hominid brain. In: Henke W, Tattersall I, editors. *Handbook of paleoanthropology.* Berlin: Springer-Verlag; 2015. p. 1961–87. doi: 10.1007/978-3-642-39979-4_81
36. Holloway R. Evolution of the human brain. In: Lock A, Peters CR, editors. *Handbook of human symbolic evolution.* Oxford: Clarendon Press; 1996. p. 74–116.
37. Wu X, Schepartz LA, Liu W. A new *Homo erectus* (Zhoukoudian V) brain endocast from China. *Proc R Soc B.* 2010;277:337–44. doi: 10.1098/rspb.2009.0149
38. Holloway RL, Hurst SD, Garvin HM, Schoenemann PT, Vanti WB, Berger LR, et al. Endocast morphology of *Homo naledi* from the Dinaledi Chamber, South Africa. *Proc Natl Acad Sci USA.* 2018;115:5738–43. doi: 10.1073/pnas.1720842115
39. Bruner E, Grimaud-Hervé D, Wu X, de la Cuétara JM, Holloway R. A paleoneurological survey of *Homo erectus* endocranial metrics. *Quat Int.* 2014;368:80–87. doi: 10.1016/j.quaint.2014.10.007
40. Falk D, Hildebolt C, Smith K, Morwood MJ, Sutikna T, Brown P, et al. The brain of LB1, *Homo floresiensis*. *Science.* 2005;308:242–5. doi: 10.1126/science.1109727
41. Gilbert WH, Holloway RL, Kubo D, Kono RT, Suwa G. Tomographic analysis of the Daka calvaria. In: Gilbert WH, Asfaw B, editors. *Homo erectus.* Pleistocene evidence from the Middle Awash, Ethiopia. Berkeley: University of California Press; 2009. p. 329–47. doi: 10.1525/california/9780520251205.003.0014
42. Ascenzi A, Biddittu I, Cassoli PF, Segre AG, Segre-Naldini E. A calvarium of late *Homo erectus* from Ceprano, Italy. *J Hum Evol.* 1996;31:409–23. doi: 10.1006/jhev.1996.0069
43. Bruner E, Manzi G, Holloway R. Krapina and Saccopastore: endocranial morphology in the Pre-Würmian Europeans. *Period Biol.* 2006;108:433–41.
44. Recheis W, Macchiarelli R, Seidler H, Weaver DS, Schäfer K, Bondioli L, et al. Re-evaluation of the endocranial volume of the Guattari 1 Neandertal specimen (Monte Circeo). *Coll Antropol.* 1999;23:397–405.
45. Kochiyama T, Ogihara N, Tanabe HC, Kondo O, Amano H, Hasegawa K, et al. Reconstructing the Neanderthal brain using computational anatomy. *Sci Rep.* 2018;8:6296. doi: 10.1038/s41598-018-24331-0
46. Henke W, Tattersall I, editors. *Handbook of paleoanthropology.* Berlin: Springer-Verlag; 2015.
47. Maddison W, Maddison D. MESQUITE: a modular system for evolutionary analysis. 2019 [cited 2024 Dec 10]. Available from: <https://www.mesquiteproject.org/>
48. Bruner E, Beaudet A. The brain of *Homo habilis*: three decades of paleoneurology. *J Hum Evol.* 2023;174:103281. doi: 10.1016/j.jhevol.2022.103281
49. Holloway RL. Human brain endocasts, Taung, and the LB1 hobbit brain. In: Broadfield D, Yuan M, Schick K, Toth N, editors. *The human brain evolving: paleoneurological studies in honor of Ralph L. Holloway.* Vol. 4. Gosport (IN): Stone Age Institute Publication Series; 2010. p. 51–58.
50. Tartarelli G. Encephalizations and cerebral developments in genus *Homo*. *Hum Evol.* 2006;21:321–35. doi: 10.1007/s11598-006-9032-7
51. Labra N, Mounier A, Leprince Y, Rivière D, Didier M, Bardin E, et al. What do brain endocasts tell us? A comparative analysis of the accuracy of sulcal identification by experts and perspectives in palaeoanthropology. *J Anat.* 2024;244:274–96. doi: 10.1111/joa.13966
52. Harmand S, Lewis JE, Feibel CS, Lepre CJ, Prat S, Lenoble A, et al. 3.3-million-year-old stone tools from Lomekwi 3, West Turkana, Kenya. *Nature.* 2015;521:310–15. doi: 10.1038/nature14464
53. Susman RL. Hand of *Paranthropus robustus* from Member 1, Swartkrans: fossil evidence for tool behavior. *Science.* 1988;240:781–4. doi: 10.1126/science.3129783
54. Dutton P, Chapman H. New tools suggest local variation in tool use by a montane community of the rare Nigeria-Cameroon chimpanzee, *Pan troglodytes ellioti*, in Nigeria. *Primates.* 2014;26:89–100. doi: 10.1007/s10329-014-0451-1
55. Anders-Bray TC, Gonder MK. Quantitative ethnography reveals behavioral elements associated with problem-solving in wild chimpanzee tool-use. In: Kim YJ, Swiecki Z, editors. *Advances in quantitative ethnography.* Berlin: Springer Verlag; 2024. p. 35–49.
56. Bruner E, Battaglia-Mayer A, Caminiti C. The parietal lobe evolution and the emergence of material culture in the human genus. *Br Struct Funct.* 2023;228:145–67. doi: 10.1007/s00429-022-02487-w
57. Berlucchi G, Vallar G. The history of the neurophysiology and neurology of the parietal lobe. *Handb Clin Neurol.* 2018;151:3–30. doi: 10.1016/B978-0-444-63622-5.00001-2
58. Bisley JW. Parietal lobe. In: Vonk J, Shackelford TK, editors. *Encyclopedia of animal cognition and behavior.* Heidelberg: Springer; 2017. p. 1–5.
59. Holloway RL. The poor brain of *Homo sapiens neanderthalensis*: see what you please. In: Delson E, editor. *Ancestors: The hard evidence.* New York: Liss; 1985. p. 319–24.
60. Holloway RL. How much larger is the relative volume of area 10 of the prefrontal cortex in humans? *Am J Phys Anthropol.* 2002;118:399–401. doi: 10.1002/ajpa.10090
61. Bookstein F, Schäfer K, Prossinger H, Seidler H, Fieder M, Stringer C, et al. Comparing frontal cranial profiles in archaic and modern *Homo* by morphometric analysis.

- Anat Rec. 1999;257:217–24. doi: 10.1002/(SICI)1097-0185(19991215)257:6%3C217::AID-AR7%3E3.O.CO;2-W
62. Bruner E, Holloway RL. A bivariate approach to the widening of the frontal lobes in the genus *Homo*. *J Hum Evol.* 2010;58:138–46. doi: 10.1016/j.jhevol.2009.10.005
63. Bruner E. Evolving Human Brains: Paleoneurology and the Fate of Middle Pleistocene. *J Archaeol Method Theory.* 2021;28:76–94. doi: 10.1007/s10816-020-09500-8
64. Pearce E, Stringer C, Dunbar RIM. New insights into differences in brain organization between Neanderthals and anatomically modern humans. *Proc Roy Soc B.* 2013;280:1758. doi: 10.1098/rspb.2013.0168
65. Semendeferi K, Damasio H. The brain and its main anatomical subdivisions in living hominoids using magnetic resonance imaging. *J Hum Evol.* 2000;38:317–32. doi: 10.1006/jhevol.1999.0381
66. García-Taberero A, Peña-Melián A, Rosas A. Primary visual cortex in neandertals as revealed from the occipital remains from the El Sidrón site, with emphasis on the new SD-2300 specimen. *J Anat.* 2018;233:33–45. doi: 10.1111/joa.12812
67. Neubauer S, Gunz P, Scott NA, Hublin J-J, Mitteroecker P. Evolution of brain lateralization: A shared hominid pattern of endocranial asymmetry is much more variable in humans than in great apes. *Sci Adv.* 2020;6:eaax9935. doi: 10.1126/sciadv.aax9935
68. Pearson A, Bruner E, Polly PD. Updated imaging and phylogenetic comparative methods reassess relative temporal lobe size in anthropoids and modern humans. *Am J Biol Anthropol.* 2023;180:768–76. doi: 10.1002/ajpa.24712
69. Rilling JK, Seligman RA. A quantitative morphometric comparative analysis of the primate temporal lobe. *J Hum Evol.* 2002;42:505–33. doi: 10.1006/jhevol.2001.0537
70. Zilhao J. The Middle Palaeolithic revolution: the origins of art, and the epistemology of paleoanthropology. In: Díaz-del-Río P, Lillios K, Sastre I, editors. *The matter of prehistory: papers in honor of Antonio Gilman Guillén*. Madrid: Consejo Superior de Investigaciones Científicas; 2020. p. 85–104.
71. Falk D. Interpreting sulci on hominin endocasts: old hypotheses and new findings. *Front Hum Neurosci.* 2014;8:134. doi: 10.3389/fnhum.2014.00134
72. Holloway RL. The human brain evolving: a personal retrospective. *Annu Rev Anthropol.* 2008;37:1–19. doi: 10.1146/annurev.anthro.37.081407.085211
73. Malikovic A, Vucetic B, Milisavljevic M, Tosevski J, Sazdanovic P, Milojevic B, et al. Occipital sulci of the human brain: variability and morphometry. *Anat Sci Int.* 2012;87:61–70. doi: 10.1007/s12565-011-0118-6
74. Allen JS, Bruss J, Damasio H. Looking for the lunate sulcus: a magnetic resonance imaging study in modern humans. *Anat Rec.* 2006;288A:867–76. doi: 10.1002/ar.a.20362